


Article

Small AntiMicrobial Peptide with In Vivo Activity Against Sepsis

Héloïse Boulet¹, Fayçal Bentot¹, Arnaud Hequet², Carine Ganem-Elbaz², Chérine Bechara¹, Emeline Pacreau³, Pierre Launay³ , Sandrine Sagan¹ , Claude Jolivalt², Claire Lacombe^{1,4}, Roba Moumné¹ and Philippe Karoyan^{1,5,6,*} 

¹ Sorbonne Université, École Normale Supérieure, PSL University, CNRS, Laboratoire des Biomolécules, LBM, 75005 Paris, France; hel.boulet@gmail.com (H.B.); faycal.bentot@gmail.com (F.B.); cherine.bechara@umontpellier.fr (C.B.); sandrine.sagan@sorbonne-universite.fr (S.S.); claire.lacombe.s@gmail.com (C.L.); roba.moumne@sorbonne-universite.fr (R.M.)

² Laboratoire Charles Friedel, UMR7223, École Nationale Supérieure de Chimie de Paris, 11 rue Pierre et Marie Curie, 75005 Paris, France; arhequet@gmail.com (A.H.); carine.ganem-elbaz@curie.fr (C.G.-E.); claude.jolivalt@sorbonne-universite.fr (C.J.)

³ Inserm U1149, Labex Inflammex, Bichat Medical School, 75005 Paris, France; emeline.pacreau@inserm.fr (E.P.); pierre.launay@inserm.fr (P.L.)

⁴ Faculté des Sciences et Technologie, Univ Paris Est-Créteil Val de Marne, 94000 Créteil, France

⁵ Kayvisa, AG, Industriestrasse, 44, 6300 Zug, Switzerland

⁶ Kaybiotix, GmbH, Zugerstrasse 32, 6340 Baar, Switzerland

* Correspondence: philippe.karoyan@sorbonne-universite.fr; Tel.: +33-44274469

Academic Editors: Henry Mosberg, Tomi Sawyer and Carrie Haskell-Luevano
Received: 30 March 2019; Accepted: 17 April 2019; Published: 1 May 2019



Abstract: Antimicrobial peptides (AMPs) are considered as potential therapeutic sources of future antibiotics because of their broad-spectrum activities and alternative mechanisms of action compared to conventional antibiotics. Although AMPs present considerable advantages over conventional antibiotics, their clinical and commercial development still have some limitations, because of their potential toxicity, susceptibility to proteases, and high cost of production. To overcome these drawbacks, the use of peptides mimics is anticipated to avoid the proteolysis, while the identification of minimalist peptide sequences retaining antimicrobial activities could bring a solution for the cost issue. We describe here new polycationic β -amino acids combining these two properties, that we used to design small dipeptides that appeared to be active against Gram-positive and Gram-negative bacteria, selective against prokaryotic versus mammalian cells, and highly stable in human plasma. Moreover, the in vivo data activity obtained in septic mice reveals that the bacterial killing effect allows the control of the infection and increases the survival rate of cecal ligation and puncture (CLP)-treated mice.

Keywords: polycationic β -amino acids; small antimicrobial peptides; sepsis

1. Introduction

If the discovery of antibiotics is one of the major medical breakthroughs of the last century, bacterial resistance has consecutively emerged as a main medical problem [1]. Indeed, the number of infections caused by bacterial strains resistant to conventional antibiotics is rising and despite the success of genomics in identifying new essential bacterial genes, there is a lack of sustainable leads in antibacterial drug discovery to address these increasing multidrug-resistant (MDR) microorganisms [2]. The search for novel antibiotics with original mechanism of action is of particular interest. In this context, Antimicrobial Peptides (AMPs) are considered as an inspirational source for future antibiotics [3,4]. Indeed, although their mechanism of action is still a matter of basic research, it is generally admitted

that most of them act directly on the bacterial membrane (membranolytic) and thus likely escape the mechanisms of bacterial resistance [5]. Although AMPs present considerable advantages as new generation antibiotics, their development as therapeutics is still limited by peptide drawbacks, such as their potential toxicity, susceptibility to proteases, and high manufacturing costs. To overcome these limitations, different strategies have been investigated: The use of unnatural amino acids is anticipated to enhance their proteolytic stability [6], while the identification of small antimicrobial peptides (SAMP) [7] with sequence length ranging from 2 to 10 amino acids is suggested as an interesting solution for the cost issue. Small non-peptidic scaffolds that mimic their mechanism of action have also been recently reported [8,9].

AMPs are usually amphiphilic sequences and contain several basic residues, i.e., lysine and arginine, as well as a hydrophobic core, which are critical for their activity. The lysine and arginine side-chains are positively charged at physiological pH and direct these amphiphilic peptides to the anionic surface of bacterial cell membranes, allowing the interaction of hydrophobic residues with the hydrocarbon core of the lipid bilayer. In the aim of identifying minimalist sequence that act like AMP, the use of building blocks bearing multi-cationic groups at physiological pH could be an interesting strategy. Aussedat et al. have previously reported a small achiral tetravalent template, the “ α -bis-arginine”, which contains twice the side chain of arginine, and thus increases the charge density of the peptide sequence [10]. Although a promising tool, the steric hindrance of the α -bis-arginine quaternary center adjacent to the amine and acid functions rendered its peptidic coupling difficult in SPPS or LPPS (Solid and Liquid Phase Peptide Syntheses). The use of additional non-bulky spacers such as glycine or β -alanine residues was necessary to incorporate this α -amino acid into peptides. Consequently, even if the number of charged residues could be reduced through the use of this multi-charged amino acid, the overall size of the peptide cannot be shortened. We report here new residues that combine the advantage of the α -bis-arginine but can be easily oligomerized leading to small peptides with potential therapeutic applications: the $\beta^{2,2}$ - and $\beta^{3,3}$ -*homo*-bis-arginine derivatives, homologated respectively on the carboxylate or on the amino side (Figure 1). We postulated that the additional methylene group of β -amino acids (in green in Figure 1) would limit the steric hindrance around the quaternary center (in red in Figure 1) and facilitate their incorporation into peptides. Oligomers of β -amino acids represent one of the most studied class of foldamers. Since the pioneer work of Seebach et al. [11], only few studies dealing with $\beta^{2,2}$ - or $\beta^{3,3}$ -amino acids have been reported in the literature [12–14]. Noticeably, while the use of lipophilic $\beta^{2,2}$ -amino acids has proven valuable for the design of both antibacterial [15] and anticancer peptides [16,17], geminally disubstituted residues with basic side-chains have not been reported so far.

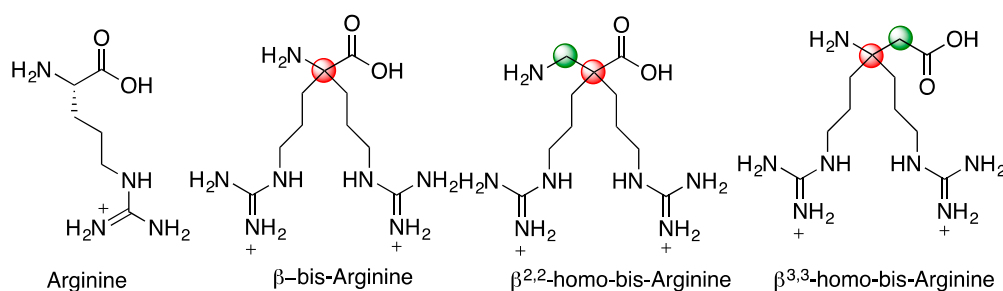


Figure 1. Bis-disubstituted-arginine analogues.

We report here the syntheses of $\beta^{2,2}$ - and $\beta^{3,3}$ -bis-*homo*-ornithine/arginine, and their use to design small cationic peptides. These peptides were evaluated as antimicrobial agents against Gram-positive and Gram-negative bacteria, and their cytotoxicity against eukaryotic cells as well as their stability in human serum were assessed. This work led to the selection of a dipeptide as a lead for in vivo studies for the treatment of sepsis in mice. Remarkably, the in vivo results revealed that the bacterial killing effect of this cationic dipeptide allows the control of the infection and sustains the immune response in the remediation of sepsis.

2. Results

2.1. Amino Acids Syntheses

The $\beta^{2,2}$ - (**1** and **2**) and $\beta^{3,3}$ -bis-*homo*-ornithine derivatives (**3**) required for the synthesis of the cationic dipeptides were prepared suitably protected for dipeptide syntheses (Figure 2).

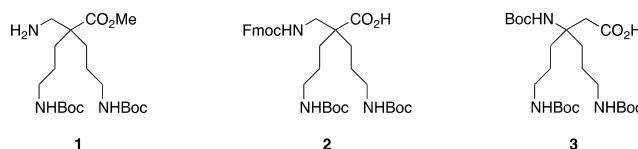
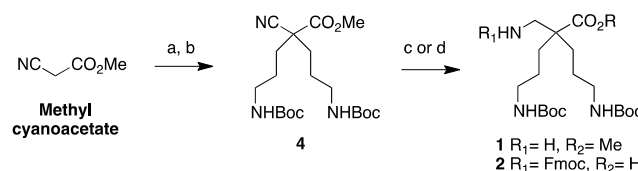


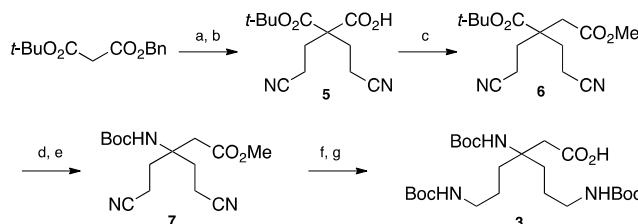
Figure 2. $\beta^{2,2}$ - and $\beta^{3,3}$ -bis-*homo*-ornithine derivatives suitably protected for peptide syntheses.

The $\beta^{2,2}$ -*homo*-bis-ornithine methyl ester **1** and the Fmoc-protected $\beta^{2,2}$ -*homo*-bis-ornithine **2** were both obtained from methyl cyanoacetate, respectively, in three and four steps (Scheme 1).



Scheme 1. $\beta^{2,2}$ -*homo*-bis-ornithine derivatives **1** and **2** syntheses. (a) $\text{CH}_2=\text{CHCN}$, LiClO_4 , NEt_3 (93%); (b) H_2 , PtO_2 , Boc_2O , MeOH (21%); (c) H_2 , Ni Raney, MeOH (**1**, 98%); (d) $1/\text{H}_2$, Ni Raney, NaOH (2 M), THF/EtOH 2/ FmocOSu , K_2CO_3 , H_2O , dioxane (**2**, 72%).

The double Michael addition on acrylonitrile [18] followed by selective reduction of the nitrile groups in γ -position over PtO_2 and simultaneous Boc-protection of the resulting amines gave the key intermediate **4** with moderate yields (21%). Improvement of this yield could be realized using a large excess of Raney Nickel (50% Yields) but was not relevant for safety reason and large-scale synthesis. Reduction of the α -nitrile by Raney nickel catalyzed hydrogenation in methanol led to the amine-free, acid-protected $\beta^{2,2}$ -*homo*-bis-ornithine derivative **1** that could be directly used in peptide coupling on the amine side. The *N*-protected, acid-free counterpart **2** was obtained when the reduction of **4** was performed in the presence of sodium hydroxide, followed by a Fmoc-protection. Boc-protected $\beta^{3,3}$ -*homo*-bis-ornithine derivative **3** was obtained starting from *tert*-butyl benzyl malonate (Scheme 2).



Scheme 2. $\beta^{3,3}$ -*homo*-bis-ornithine derivatives **3** synthesis. (a) $\text{CH}_2=\text{CHCN}$ LiClO_4 , NEt_3 (88%); (b) $\text{NH}_4^+\text{HCO}_2^-$, Pd/C , MeOH (83%); (c) 1/1-chloro-*N,N*,2-trimethyl-1-propenylamine, DCM 2/ TMSCHN_2 , DIEA , CH_3CN 3/ Ag_2O , DMF/MeOH , reflux (21%); (d) $\text{TFA}/\text{TIS}/\text{DCM}$ (86%); (e) 1/ ClCO_2Et , NEt_3 , acetone, 0°C 2/ NaN_3 , H_2O 3/ toluene , *tert*- BuOH , reflux (35%); (f) 1/ PtO_2 , H_2 , $\text{CHCl}_3/\text{MeOH}$ 2/ K_2CO_3 , Boc_2O , $\text{H}_2\text{O}/\text{THF}$ (62%); (g) LiOH , $\text{CH}_3\text{CN}/\text{H}_2\text{O}$ (98%).

The double Michael addition on acrylonitrile followed by selective benzyl ester hydrogenolysis using ammonium formate on palladium charcoal gave compound **5**. Arndt–Eistert homologation catalyzed by silver oxide led to compound **6** with 21% yields over the three steps. After deprotection of the *t*-Bu ester, the acid group was converted to Boc-protected amine via a Curtius rearrangement. Reduction of the nitrile groups in γ -position was then achieved by platinum oxide catalyzed

hydrogenation. Finally, protection of the amino groups as Boc-carbamate and saponification of the methyl ester gave access to compound **3** readily usable for peptide coupling on the acid side.

2.2. Peptides Design and Syntheses

With these compounds in hand, we have designed antimicrobial dipeptides inspired by the work of Svendsen and co-workers, who defined the minimal set of functional motifs required to develop short AMPs as two cationic charges and two bulky hydrophobic aromatic units [19,20]. Based on this minimalist pharmacophore model, they indeed developed promising antibacterial tripeptides composed of a central 2,5,7-tri-tertbutyltryptophan (Tbt) flanked by two arginine residues. These peptides have anti-infectious properties and have reached phase-II clinical studies [21–23]. Several other groups have then reported the successful implementation of this pharmacophore model [24–26]. Starting from the peptide reported by Svendsen et al., the two arginine residues were replaced by one dicationic amino acid, leading to dipeptides **8–13** containing a tryptophan derivative (Trp or Tbt) and a dicationic $\beta^{2,2}$ - or $\beta^{3,3}$ -amino acid: Trp- $\beta^{2,2}$ -*h*-bis-Orn-OMe (**8**), Tbt- $\beta^{2,2}$ -*h*-bis-Orn-OMe (**9**), Gdm-Trp- $\beta^{2,2}$ -*h*-bis-Arg-OMe (**10**), Tbt- $\beta^{2,2}$ -*h*-bis-Arg-OMe (**11**), Gdm-Tbt- $\beta^{2,2}$ -*h*-bis-Arg-OMe (**12**), and $\beta^{3,3}$ -*h*-bis-Arg-Tbt-OMe (**13**) (Figure 3). In order to investigate the effect of the positive charge segregation on the antimicrobial activity of the compound [27], we also synthesized peptide **14** (Gdm- $\beta^{2,2}$ -*h*-bis-Arg-Tbt-OMe), in which the sequence of dipeptide **11** is reversed.

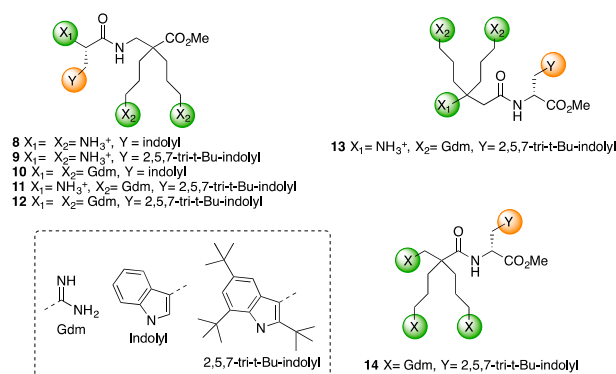
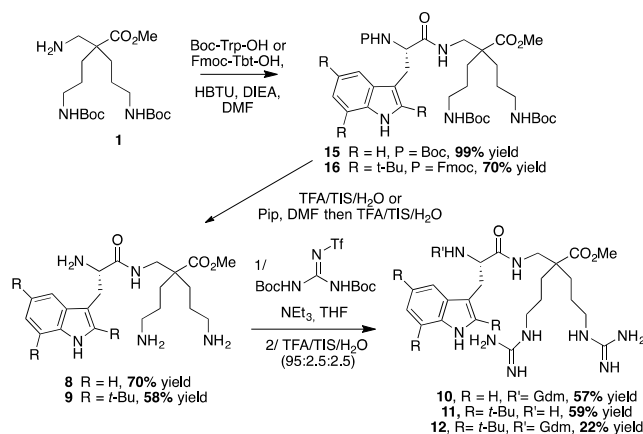


Figure 3. Structure of polycationic dipeptides **8–14**.

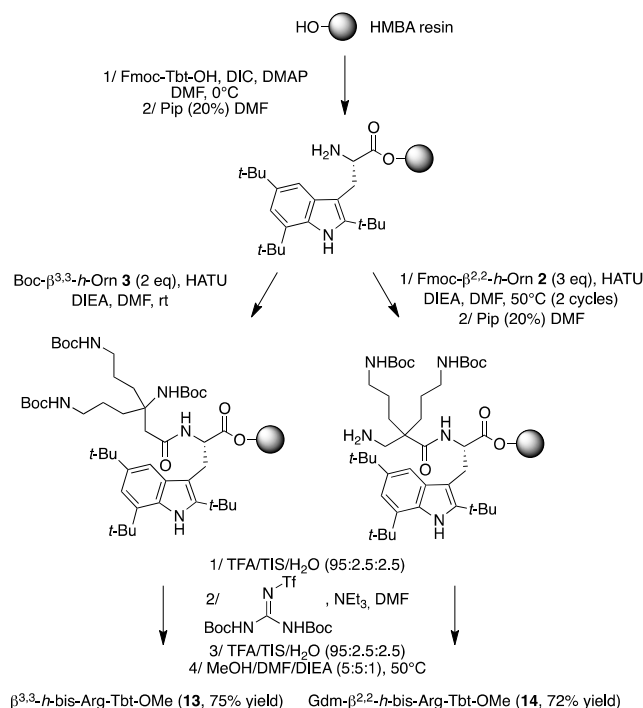
To evaluate the ease of coupling of these new beta derivatives against their alpha counterparts, both liquid and solid phase peptide syntheses were tested. Compounds **8–12** were prepared by coupling the corresponding tryptophan derivatives (Boc-Trp-OH or Fmoc-Tbt-OH) with the $\beta^{2,2}$ -*h*-bis-ornithine methyl ester **1** in solution, using HBTU as a coupling agent, in the presence of DIEA, in DMF (Scheme 3).



Scheme 3. Synthesis of peptides **8–12** by LPPS.

The fully protected dipeptides **15** and **16** were obtained from Boc-Trp-OH and Fmoc-Tbt-OH, in respectively 99% and 70% yields. Noticeably, the α -bis-ornithine derivative coupling failed in the same conditions. Deprotection of the amines gave access to the corresponding $\beta^{2,2}$ -*h*-bis-Ornithine derivatives **8** and **9**. Introduction of the guanidinium group (Gdm) on these two compounds followed by Boc-deprotection using a TFA cocktail led to the $\beta^{2,2}$ -*h*-bis-Arg derivatives. While a unique tri-guanylated compound was obtained for the tryptophan containing dipeptide **10**, two products were isolated for the Tbt-derived compound in respectively 59% and 22% yields: One with the guanidinium groups on the side chains of the amino acids (**11**) only, and one with an additional guanidinium group on the β -amine (**12**).

The synthesis of peptides **13** and **14** was achieved by SPPS, starting from a HMBA resin-bound Tbt (Scheme 4).



Scheme 4. Synthesis of peptides **13** and **14** by SPPS.

In both cases coupling of Fmoc- $\beta^{2,2}$ -*h*-bis-Orn-OH **2** and Boc- $\beta^{3,3}$ -*h*-bis-Orn-OH **3** was achieved through HATU activation, in the presence of DIEA, in DMF. However, because of the steric hindrance of its carboxyl group, heating at 50 °C as well as a second coupling round were necessary to ensure the complete conversion of **2**. As anticipated, the improved reactivity of the carboxyl group of this residue with its $\beta^{3,3}$ -counterpart confirms that an additional methylene near the quaternary center is an effective strategy to facilitate the incorporation of the bis-ornithine derivative into a peptide sequence. After piperidine-mediated Fmoc-deprotection and/or removal of the acid labile protective groups by treatment with a trifluoroacetic acid (TFA)-triisopropylsilane (TIS)-H₂O cocktail, introduction of the guanidine moiety was performed using an excess of 1,3-di-Boc-2-(trifluoromethylsulfonyl)guanidine in DMF, in the presence of triethylamine, followed by removal of the Boc-protective groups. Cleavage of peptides **13** and **14** from the resin was achieved by treatment with methanol in the presence of DIEA and DMF giving direct access to the methyl ester protected dipeptide. Compound **14** was obtained as a tri-guanylated derivative. On the contrary, as expected, the steric hindrance of the quaternary β -amino group of compound **13** prevents any reaction on the backbone amine. In addition, NMR analysis confirmed that peptide **13** was only guanylated on the amine side-chains. Several studies have reported that the N-terminal capping of cationic peptides with a fatty acid moiety enhances their antimicrobial activity [28,29]. Thus, in order to further improve the potency of **11**, an additional

hydrophobic group was incorporated, first on the N-terminal end of the sequence. (Figure 4, peptides 17–19).

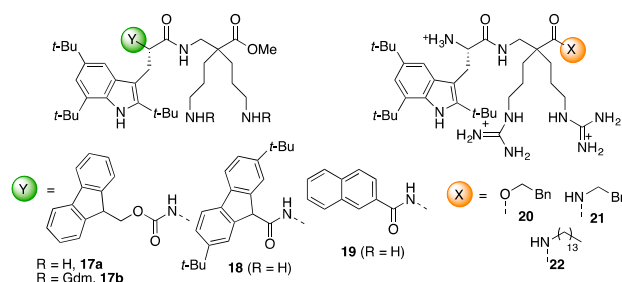


Figure 4. Pharmacomodulation of antimicrobial peptide.

We also evaluated whether such a capping effect could be also observed in this series of peptides. The biological activities of Fmoc-protected derivatives Fmoc-Tbt-β^{2,2}-h-bis-Orn-OMe **17a** and Fmoc-Tbt-β^{2,2}-h-bis-Arg-OMe **17b** were synthesized in addition to the ones of the two compounds **18** and **19** capped through a more robust amide bond at their N-terminal end. All peptides were purified to >95% homogeneity by preparative RP-HPLC and the mass of each purified peptide was checked by MALDI MS (see Supporting Information).

Finally, in order to study the influence Trp- and Tbt derivatives, we compared the retention time in RP-HPLC of selected peptides (Figure 5).

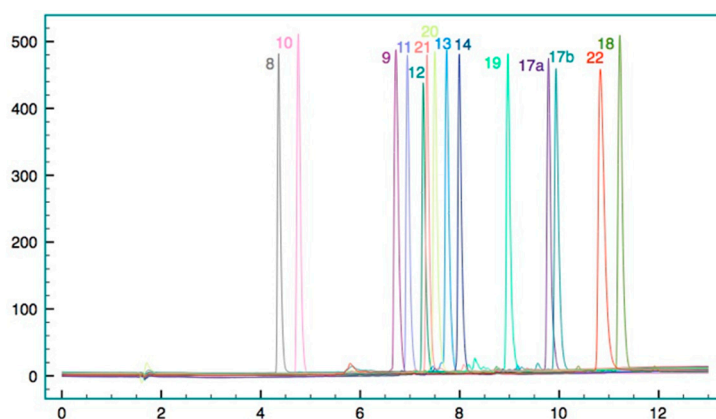


Figure 5. Superimposition of the analytical HPLC of peptides **8** to **22** on a C18 column, using as eluting gradient H₂O containing 0.1% TFA with 5% to 100% with MeCN containing 0.1% TFA.

2.3. Biological Activities

2.3.1. Antimicrobial, Hemolytic, and Cytotoxic Activities and Serum Stability

The antibacterial activities of the peptides were then investigated in the conditions reported by Svendsen, by determining the Minimal Inhibitory Concentration (MIC, µg/mL) on six strains of bacteria; three Gram-positive, *Staphylococcus aureus* ATCC25923, *Enterococcus faecalis* ATCC29212, and the methicillin resistant *Staphylococcus aureus* SA-1199B, and three Gram-negative, *Escherichia coli* ATCC25922, *Pseudomonas aeruginosa* ATCC27853, and *Acinetobacter baumannii* ATCC19606 [14] (Table 1). The tri-peptide Arg-Tbt-Arg-NH₂ reported by Svendsen (called here peptide A), and the dipeptide Tbt-Arg-OMe (called here peptide B), were used as positive controls of our experimental conditions.

The hemolytic and cytotoxic activities against human cells of all active peptides were assessed (Table 1, Figures 6 and 7 and Supporting Information).

Table 1. Biological activity, hemolytic activities, and cytotoxicity.

	MIC in µg/mL (µM)						% Hemolysis		% Cytotoxicity ^a	
	<i>S. aureus</i> ATCC25923	<i>S. aureus</i> 1199B	<i>E. faecalis</i> ATCC29212	<i>E. coli</i> ATCC25922	<i>P. aeruginosa</i> ATCC27853	<i>A. baumannii</i> ATCC19606	10 µM	50 µM	10 µM	50 µM
A	8 (12)	16 (23)	32 (47)	>64 (>93)	32 (47)	>64 (>93)	ND	ND	ND	ND
B	8 (15)	16 (30)	16 (30)	>64 (>120)	>64 (>120)	>64 (>120)	ND	ND	ND	ND
8	>64 (>16)	>64 (16)	>64 (>16)	>64 (>16)	>64 (>16)	>64 (>16)	ND	ND	ND	ND
9	8 (14)	>64 (112)	>64 (112)	>64 (112)	>64 (112)	>64 (112)	ND	ND	ND	ND
10	64 (120)	>64 (120)	>64 (120)	>64 (120)	>64 (120)	>64 (120)	ND	ND	ND	ND
11	2 (3)	16 (24)	16 (24)	8 (12)	4 (6)	64 (97)	<1	20	<1	<1
12	2 (3)	8 (12)	8 (12)	2 (3)	2 (3)	64 (92)	<1	30	<1	<1
13	2 (3)	2 (3)	4 (6)	8 (12)	8 (12)	>64 (97)	<1	10	<1	<1
14	8 (12)	8 (12)	8 (12)	32 (46)	>64 (92)	64 (92)	<1	20	<1	<1
17a	4 (5)	2 (2.5)	2 (2.5)	>64 (80)	>64 (80)	4 (5)	80	ND	45	85
17b	4 (4)	2 (2)	2 (2)	>64 (73)	>64 (73)	4 (4)	70	ND	10	80
18	8 (9)	8 (9)	8 (9)	>64 (73)	>64 (73)	64 (73)	20	ND	50	80
19	2 (3)	2 (3)	2 (3)	8 (11)	16 (22)	32 (44)	25	ND	55	80
20	1 (1.5)	2 (3)	2 (3)	2 (3)	8 (11)	8 (11)	2	30	<1	55
21	2 (3)	4 (6)	8 (11)	8 (11)	>64 (88)	8 (11)	5	30	<1	<1
22	32 (48)	>64 (96)	>64 (96)	>64 (96)	>64 (96)	>64 (96)	ND	ND	ND	ND

Minimal inhibitory concentrations (MIC in µg/mL) were measured against three Gram-positive (*S. aureus* ATCC25923, *S. aureus* 1199B, and *E. faecalis* ATCC29212) and three Gram-negative strains (*E. coli* ATCC25922, *P. aeruginosa* ATCC27853, and *A. baumannii* ATCC19606). Hemolytic activity against juvenile rat cells (Figure 6) and cytotoxicity against human SHSYS5 cells (Figure 7) were measured after incubation of the peptides at 10 and/or 50 µM, respectively for one and three hours. ND: not determined.

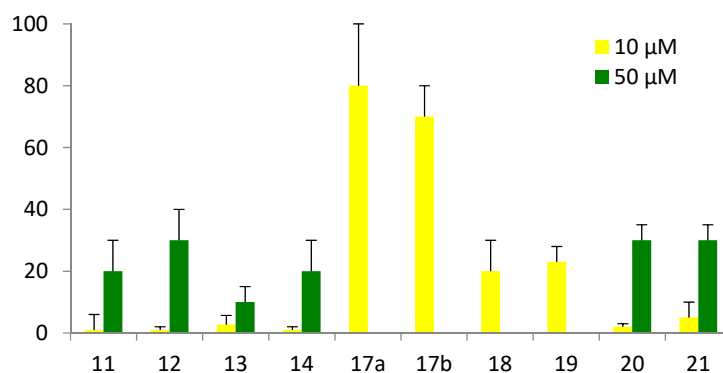


Figure 6. Percentage of hemolysis (see Supporting Information). The given results correspond to a percentage calculated as follows: %age = absorbance obtained with the peptide - absorbance obtained with the negative control (=buffer alone)/absorbance obtained with the positive control (=triton). * The haemolytic activities of peptides 17a, 17b, 18, and 19 were not measured at 50 µM because of their poor solubility at such concentration.

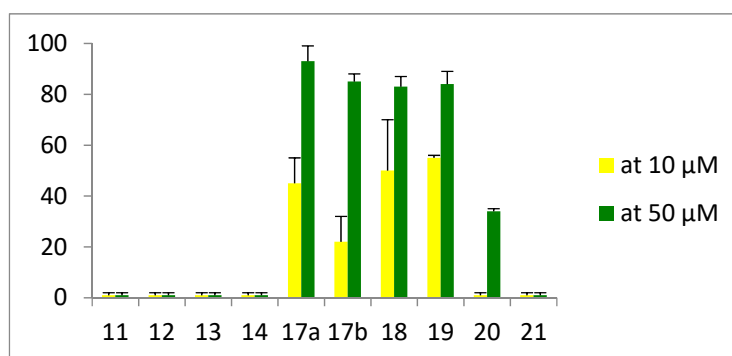


Figure 7. Percentage of cell death (see Supporting Information).

2.3.2. Interaction with Membrane Model

Although the mechanism of action of AMPs is still an active field of research, it is generally admitted that a common primary mode of action involves the disruption of cellular membrane. In order to get some insights into the mechanism of action, biophysical studies were conducted with membrane model. We used the intrinsic fluorescent properties of the tryptophan residue, as initial analysis of the bactericidal mechanism [30]. Depending on its environment in peptides, the wavelength of the fluorescence light emitted by the aromatic tryptophan residues varies. In a polar environment (water), λ_{max} is circa 357 nm, whereas in a non-polar one, λ_{max} shifts to shorter wavelengths (blue-shift). Moreover, the emission intensity increases when the tryptophan residue enters into a hydrophobic environment [31]. We therefore recorded the fluorescence of the most active peptide **11** and compared it to the inactive one **10** (Figure 8).

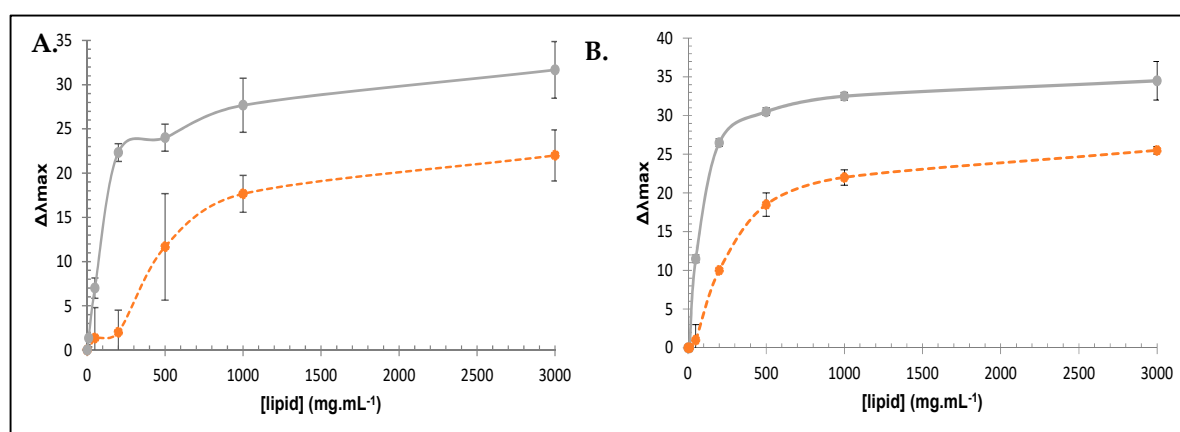


Figure 8. Lipid-induced changes in tryptophan fluorescence of peptide **11** (full line) and **10** (dashed line). Blue-shift for tryptophan in the wavelength of maximal emission in the presence of large unilamellar vesicles (LUVs) produced from *S. aureus* ATCC25923' phospholipids (A) and from *E. coli* K12 (B) (see Supporting Information).

2.3.3. In Vivo Experiment Studies

In vivo experiment studies were conducted on septic mice. Sepsis is a life-threatening condition described as a syndrome of infection complicated by acute organ dysfunction. It is still a leading cause of death in intensive care units despite early antibiotic strategies to control bacterial infection [32]. Therefore, the rapidity and efficacy of antibacterial strategies are highly connected to the outcome of this acute disease and patient survival. After acute cecal ligation and puncture (CLP), peptide **11** or PBS (negative control) were injected to mice and survival was observed (Figure 9).

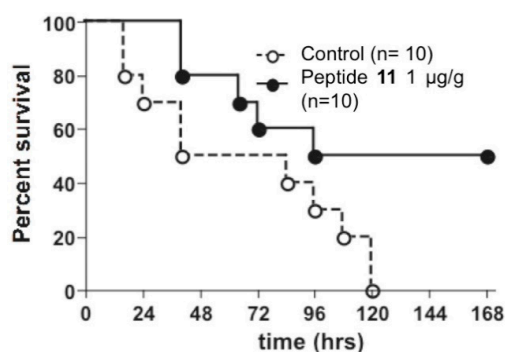


Figure 9. Survival after acute cecal ligation and puncture (CLP) in PBS-injected mice (open circle; n = 10) and peptide 11-injected mice (closed circle; n = 10). Kaplan–Meier curves and log-rank test were used to analyze the mortality rate; P = 0.0299.

3. Discussion

We have designed small AMPs based on new polycationic β -amino acids, $\beta^{2,2}$ - and $\beta^{3,3}$ -*homo*-bis-ornithine derivatives. These moieties mimic the cationic side chains of two lysine residues or two arginine residues and thus allow shortening the cationic AMP size. Their combination with the supertryptophan residue (2,5,7-tri-*tert*butyltryptophane) reported by Svendsen and co-workers allows obtaining highly active antimicrobial dipeptides. They exhibit activity in the range of 2 to 16 $\mu\text{g/mL}$ (Table 1), values that are promising for compounds to enter into clinical trials. Among the different peptides tested, several $\beta^{2,2}$ - and $\beta^{3,3}$ -*bis* cationic derivatives (peptides **11**–**14**) were potent killing agents against the different strains, with MIC values comparable to or lower than that of the positive controls, and no significant difference was observed between the compound derived from the $\beta^{2,2}$ - (**11**) and $\beta^{3,3}$ -*h*-bis-Arg (**13**). Noticeably, the $\beta^{2,2}$ -amino acid derivatives are easier to synthesize.

Some structure activity relationships can be drawn from these results. First, the importance of the guanidinium groups for the antimicrobial activity is highlighted, since peptide **9**, containing the $\beta^{2,2}$ -*h*-bis-Orn, shows little antimicrobial activity against all strains (except *S. aureus*) compared to the $\beta^{2,2}$ -*h*-bis-Arg analog **11**. This net difference in the antimicrobial activity of arginine- and lysine-containing compounds agrees with the literature and is believed to result from the stronger ability of the guanidinium group to form bidentate hydrogen bonds with the phosphate moiety of phospholipid polar heads, in addition to electrostatic interactions [33]. Oppositely, the absence of difference in the antimicrobial activity of peptides **11** and **12** indicates that the additional guanidinium group on the β -amine has little influence, suggesting that the cationic group on the N-terminal end is not involved in the pharmacophore of the peptide.

Another important point is the positive influence of the *t*-Bu group on the tryptophan moiety, similar to the peptide reported by Svendsen et al. Indeed, in comparison to **11** or **12**, peptide **10** presents no activity on the tested strains. This lack of activity can be related to the lower lipophilicity of tryptophan compared to the Tbt derivatives **11** and **12**, confirmed by its lower retention time in RP-HPLC (Figure 5) together with its lower capacity to interact with membrane. Indeed, the larger size of Tbt compared to Trp (around 2.5-fold) could allow a deeper penetration of this hydrophobic residue into the phospholipid bilayer and an effective disruption of the membrane that is not allowed by the smaller indole moiety. In order to evaluate this hypothesis, we recorded the fluorescence of the active peptide **11**, and compared it to the inactive peptide **10**. The tryptophan fluorescence spectra of both peptides in aqueous buffer had a maximum emission at 355 nm. Addition of increasing concentration of large unilamellar vesicles (LUVs), prepared from phospholipids directly extracted from *S. epidermidis*, showed large blue-shift (near 35 nm) in the emission maxima of peptide **11**, characteristic of the embedding of Trp side chain into the hydrophobic medium of the negatively charged phospholipid (Figure 2). For peptide **10**, the blue-shift was 10 nm smaller with apparent binding constant K_L (lipid concentration that induced 50% of maximal blue-shift) about 3 times lower for peptide **11** ($90 \pm 2 \text{ mg}\cdot\text{mL}^{-1}$ s and $100 \pm 1.5 \text{ mg}\cdot\text{mL}^{-1}$, respectively with *S. aureus* LUVs and *E. coli* LUVs) than for peptide **10** ($280 \pm 1.5 \text{ mg}\cdot\text{mL}^{-1}$ and $500 \pm 6 \text{ mg}\cdot\text{mL}^{-1}$ with *S. aureus* LUVs and *E. coli* LUVs). These preliminary biophysical studies on the interaction of **11** with model membrane suggested that this compound indeed could act as an antimicrobial peptide, by destabilizing the bacterial membrane. We are aware that deeper investigations might be performed in order to assess the mechanism by which this membrane permeabilization occurs.

Interestingly, the sequence of the dipeptides seemed to have an influence on the bacterial activity. Indeed, even though the reverse peptide **14** had a similar activity against Gram-positive bacteria as the one of peptide **12**, its potency against some of the Gram-negative strains was significantly lower. This decreased activity was accompanied by a higher hydrophobicity according to its longer retention time on reversed-phase HPLC (Figure 5). We anticipate that since the chemical composition of these peptides is similar, these different behaviors are likely related to a different spatial arrangement of the cationic and hydrophobic side-chains, giving a different amphiphilicity to peptide **14** vs. **12**. Indeed, AMPs usually adopt facially amphiphilic conformations in which cationic hydrophilic and

hydrophobic side chains segregate onto opposite regions of the molecular surface. The importance of this overall topology and not the precise sequence, secondary structure, or chirality of the peptides has been highlighted as key features for their cell-killing activity [34]. Seminal works from Seebach [11] and more recently from Balaram [13,35] suggest that achiral $\beta^{2,2}$ -amino acids are β -turn inducers. In order to get some insight into the solution structure of these peptides, ^1H NMR studies were conducted in D_2O . Assignment of the proton signals was achieved by combination of COSY, TOCSY, and NOESY measurements. The data reveal that for peptides **9**, **11**, and **12**, one of the two β -protons CH_2NH of the $\beta^{2,2}$ -*h*bis-Arg is significantly down-field shifted (2.4, 1.8 ppm, and 2.8 ppm respectively for **9**, **11**, and **12**) compared to the other (3.5 ppm), which is not the case for peptide **14**. Moreover, the presence of the *t*Bu group on the indole moiety has an important effect on the chemical shift of this proton since for peptides **8** and **10**, the chemical shift of this proton is 3.1–3.2 ppm. Altogether, these data suggest a close proximity between the β -protons CH_2NH of the $\beta^{2,2}$ -*h*bis-Arg and the indole moiety in peptides **9**, **11**, and **12**, most likely because of cation- π interactions. Regardless of its nature, this specific conformation might favor the interaction of the peptide with the bacterial membrane and bring an explanation for the different biological behaviors of the two isomers **12** and **14** towards Gram-negative bacteria.

Regarding hemolysis (Figure 6), significant hemolytic effect was observed only at concentrations much higher than the antibacterial MIC values for the four most active peptides **11–14**, indicating a good selectivity of the compounds for bacterial cells over mammalian cells. Moreover, no cytotoxicity was observed for the 4 peptides **11–14** on human SHSYS5 cells. Finally, while introduction of fluorenyl or naphthyl group led to improved antibacterial activity for peptides **17–19**, this enhancement was, however, accompanied by a decreased selectivity on bacteria, and a significant increase in hemolysis and cytotoxicity on human cells (Table 1). We then evaluated the influence of an additional hydrophobic group on the C-terminal end (peptides **20–22**). While replacement of methyl ester with benzyl ester (**20**) or benzamide (**21**) gave peptides with enhanced efficiency, the incorporation of an alkyl chain (**22**) completely abolished the antimicrobial activity, probably reflecting an inappropriate balance between hydrophobicity and charge in this peptide.

Altogether, we selected peptide **11** as the best candidate for further analysis of its potential as therapeutic agent, thanks to its lack of haemolytic and cytolytic activity on mammalian cells and the easier synthesis of $\beta^{2,2}$ -*h*-bis-Orn-OH compared to $\beta^{3,3}$ -*h*-bis-Orn-OH. Since the incorporation of β -amino acids into peptides is known to improve their metabolic stability, the serum stability of this compound was first evaluated in human plasma (See Figure 10), where it appeared to be completely stable over 24 h, as expected for β -amino acids containing peptides sequences compared to a positive control peptide (4NKG) that was fully degraded in 20 min (See 4. Materials and Methods).

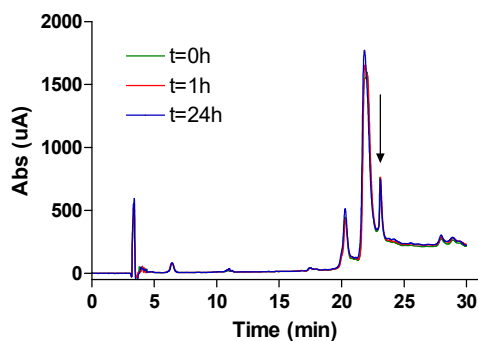


Figure 10. Serum stability of compound **11** evaluated in human plasma (See Supporting Information).

The potency of peptide **11** was finally assessed *in vivo* in septic mice. In order to analyze its potential, mice were subjected to the acute model of sepsis “high grad sepsis” in which less than 50% of the mice survived to the procedure (See SI). In our technical conditions, 100% of the CLP-induced control mice succumbed during the five days following the induction of sepsis (Figure 9). However, the mice treated with one peritoneal injection of the peptide at 1 $\mu\text{g}/\text{g}$ show a significant increase of the

survival rate. Indeed, 50% of the mice treated with peptide **11** survived the acute peritonitis. The results revealed that the injection of peptide **11** induced an increase in the survival rate of CLP-treated mice.

Finally, this study validates these polycationic residues as new tools for the design of short bioactive antimicrobial cationic peptides. These new unnatural arginine analogs might be useful tools for other applications for which cationic residues are a key player, such as cell-penetrating peptides or RNA ligands.

4. Materials and Methods

4.1. General Considerations

All reactions were carried out under argon atmosphere with dry commercial or freshly distilled solvents under anhydrous conditions unless otherwise stated. All reagents were purchased from commercial suppliers and used without further purification. Flash chromatography was performed using silica gel Merck 60 (0.040–0.063 μm , Molsheim, France). Analytical thin-layer chromatography (TLC) was performed using silica gel Merck 60 on alumina, visualized by UV fluorescence at 254 nm, and revealed with ninhydrin (0.3% in *n*-butanol/AcOH) or phosphomolybdic acid (solution in EtOH).

4.2. Solid Phase Peptide Synthesis

All reactions were carried out in Polypropylene Torviq syringes (sizes 5, 10, 20, or 50 mL) equipped with a porous polypropylene disc at the bottom and closed with an appropriate cap. HMBA resin (4-(Hydroxymethyl)benzoyl-aminoethyl) polystyrene (200–400 mesh, 0.8–1.2 mmol/g) was purchased from Iris Biotech (Marktredwitz, Germany). The loading of the Fmoc amino acid coupled resin was determined using a Cary3 UV/VIS spectrometer (Agilent, Santa-Clara, CA, USA). *O*-(Benzotriazol-1-yl)-*N,N,N',N'*-tetramethyluronium hexafluorophosphate (HBTU) and 2-(1H-9-azabenzotriazole-1-yl)-1,1,3,3-tetramethyluronium hexafluorophosphate (HATU) were purchased from Iris Biotech. Solvents were purchased from VWR in HPLC grade and used without further purification. Purifications were performed by reverse-phase HPLC either on a Waters preparative HPLC system connected to a Breeze software (Fisher Scientific, Illkirch, France), using a *Waters XBridge* column (RP C18, 19 \times 50 mm, 5 μm , 135 \AA) at a flow rate of 14 mL/min or a Dionex semi-preparative HPLC-system connected to a Chromeleon software (Fisher Scientific, Illkirch, France), using a C18 semi-preparative column from AIT at a flow rate of 5 mL/min; and using as eluent A, H₂O containing 0.1% of TFA, and as eluent B, CH₃CN containing 0.1% of TFA. UV detection was done at 220 nm and 280 nm. Purification gradients were chosen to get a ramp of approximately 1% solution B per minute in the interest area. Peptide fractions from purification were analyzed by analytical HPLC, pooled according to their purity, partly concentrated under vacuum, and freeze-dried on an Alpha 2/4 freeze dryer from Bioblock Scientific (Fisher Bioblock Scientific, Rungis, France) to get the expected peptide as a powder.

4.3. Product Characterisation

NMR spectra were recorded on Bruker ARX 250 (Bruker, France SAS, Wissembourg, France) or Bruker Avance III 300 spectrometers (Bruker, France SAS, Wissembourg, France) unless otherwise noted. Proton chemical shifts values (δ) are reported in parts per million (ppm) downfield from tetramethylsilane (TMS) unless noted otherwise. Coupling constants (*J*) are reported in Hertz (Hz). Carbon chemical shifts values (δ) are reported in parts permillion (ppm) with reference to internal solvent CDCl₃ (77.00 ppm) or CD₃OD (49.00 ppm). Multiplicities are abbreviated as follows: Singlet (s), doublet (d), triplet (t), quartet (q), multiplet (m), and broad singlet (bs). Signal assignments were made using COSY and HSQC experiments, and for peptides NOESY (250 ms mixing time), TOCSY (80 ms mixing time), and DQF-COSY spectra. High-resolution mass spectra (HRMS) were obtained on a Finnigan MAT 95 instrument and are given as experimental (found) and theoretical (calcd). Analytical RP-HPLC were performed on either a Waters system connected to a Breeze software or a Dionex system

connected to a Chromeleon software. Waters system consisted of a binary pump (Waters 1525) and a dual wavelength UV/visible Absorbance detector (Waters 2487, Saint-Quentin-en-Yveline, France). Dionex system consisted in an analytical automated LC system (Ultimate 3000) equipped with an auto sampler, a pump block composed of two ternary gradient pumps, and a dual wavelength detector. The analyses were performed on C18 analytical columns (from AIT (Paris, France) or Higgins (San Diego, CA, USA)) using as eluent A, H₂O containing 0.1% of TFA and as eluent B, CH₃CN containing 0.1% of TFA, at a flow rate of 1 mL/min. UV detection was done at 220 and 280 nm. Peptides were characterized by MALDI-TOF MS (DE-Pro, PerSeptive Biosystems, Framingham, MA, USA) in positive ion reflector mode using the matrix α -cyano-4-hydroxy-cinnamic acid (CHCA). Peptide molecular weights were determined for the free amine and not for the TFA salts.

4.3.1. Synthesis of H- $\beta^{2,2}$ hbis-Orn(Boc)₂OMe 1 and Fmoc $\beta^{2,2}$ hbis-Orn(Boc)₂OH 2 (Scheme 5)

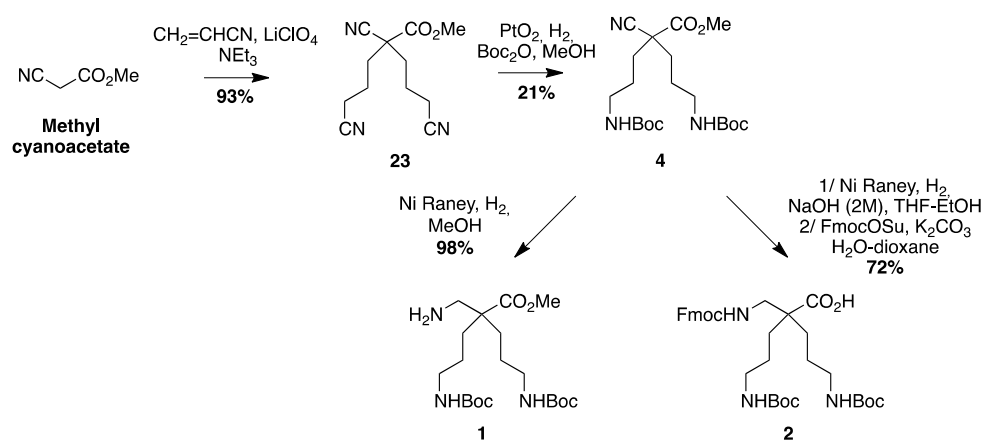
Methyl 2,4-dicyano-2-(2-cyanoethyl)butanoate 23: Methyl 2-cyanoacetate (10 g, 100 mmol) was mixed with acrylonitrile (11.7 g, 220 mmol) in a three-necked round bottom flask equipped with a condenser and an addition funnel. Triethylamine (6.8 mL, 50 mmol) was added dropwise at 0 °C through the addition funnel. The reaction was stirred continuously and allowed to react overnight at rt. After confirming completion of the reaction by TLC, AcOEt was added. The organic layer was washed with 5% citric acid solution and brine, dried over MgSO₄, filtered, and evaporated. The product precipitated overnight. The solid was washed with AcOEt and obtained as a pale yellow powder (19.27 g, 93% yield); **R_f** (Cy/AcOEt, 1:1) = 0.47; ¹H NMR (250 MHz, CDCl₃) δ 3.87 (s, 3H, CO₂CH₃), 2.37–2.62 (m, 4H, CH₂ β), 2.31 (ddd, *J* = 15.5 Hz, 8.6 Hz, 6.8 Hz, 2H, CH₂ γ), 2.14 (ddd, *J* = 14.2 Hz, 8.6 Hz, 6.1 Hz, 2H, CH₂ γ); ¹³C NMR (75 MHz, CDCl₃): δ 166.6 (C, C=O), 117.2 (2C, C \equiv N γ), 116.1 (C, C \equiv N α), 54.30 (CH₃, CO₂CH₃), 47.6 (C, C α), 32.1 (2CH₂, CH₂ β), 13.6 (2CH₂, CH₂ γ); MS-ESI+: calcd for C₁₀H₁₁N₃O₂ 205.09, calcd for C₁₀H₁₁N₃O₂Na 228.08, found 228.07 [M + Na]⁺.

Methyl 2-cyano-4-(Boc)amine-2-(3-(Boc)amine propyl)pentanoate 4: Compound **23** (10 g, 49 mmol) was dissolved in methanol (25 mL). Boc₂O (23.5 g, 108 mmol) and PtO₂ (2.2 g, 9.8 mmol) were added and the reaction mixture was stirred at rt for 3 days under 5 bars of H₂ pressure. The reaction mixture was filtered through a celite pad and evaporated to dryness. The crude compound was purified by flash chromatography (Cy/AcOEt 100:0 \rightarrow 70:30) to afford yellowish oil (5 g, 21% yield); **R_f** (Cy/AcOEt, 1:1) = 0.56; ¹H NMR (300 MHz, CDCl₃): δ (ppm) 4.69 (bs, 2H, NH), 3.76 (s, 3H, CO₂CH₃), 3.08–3.20 (m, 4H, CH₂ δ), 1.44–2 (m, 8H, CH₂ $\beta\alpha\gamma\delta$ CH₂ γ), 1.37–1.50 (m, 18H, C(CH₃)₃); ¹³C NMR (62.5 MHz, CDCl₃) δ 169.1 (C, C=O ester), 155.8 (2C, C=O carbamate), 118.7 (C, C \equiv N), 79.3 (2C, C(CH₃)₃), 53.3 (CH₃, CO₂CH₃), 49.1 (C, C α), 39.7 (2CH₂, CH₂ δ), 34.4 (2CH₂, CH₂ β), 28.2 (6CH₃, C(CH₃)₃), 26.1 (2CH₂, CH₂ γ); MS-ESI+: calcd for C₂₀H₃₅N₃O₆ 413.25, calcd for C₂₀H₃₅N₃O₆Na 436.24, found 436.24 [M + Na]⁺.

H- $\beta^{2,2}$ hbis-Orn(Boc)₂OMe 1: Compound **4** (2.35 g, 4.9 mmol) was dissolved in methanol (100 mL). Raney nickel was added, and the mixture was stirred under 5 bars of H₂ pressure at rt for 3 days. The reaction mixture was filtered through a celite pad and evaporated to dryness. The product was used in peptide synthesis without further purification. (2.0 g, 98% yield); **R_f** (Cy/AcOEt, 1:1) = 0.56; ¹H NMR (300 MHz, MeOD) δ 3.68 (s, 3H, CO₂CH₃), 3.01 (t, *J* = 6.7 Hz, 4H, CH₂ δ), 2.77 (s, 2H, CH₂ $\beta\epsilon$), 1.55–1.60 (m, 4H, CH₂ β), 1.32–1.43 (m, 22H, CH₂ γ and C(CH₃)₃); ¹³C NMR (75 MHz, MeOD) δ 177.9 (C, C=O ester), 158.6 (2C, C=O carbamate), 79.9 (2C, C(CH₃)₃), 52.4 (CH₃, CO₂CH₃), 51.5 (C, C α), 45.9 (CH₂, CH₂ $\beta\epsilon$), 41.6 (2CH₂, CH₂ δ), 31.2 (2CH₂, CH₂ β), 28.8 (6CH₃, C(CH₃)₃), 25.4 (2CH₂, CH₂ γ); HRMS-ESI+: calcd for C₂₀H₃₉N₃O₆ 417.2839, found 418.2915 [M + H]⁺.

Fmoc $\beta^{2,2}$ hbis-Orn(Boc)₂OH 2: Compound **4** (2.3 g, 5.6 mmol) was dissolved in methanol (125 mL). An aqueous solution of sodium hydroxide (2 M) (12.5 mL, 25 mmol) and Raney nickel were added. The mixture was stirred under 5 bars of H₂ pressure at rt for 7 days. The reaction mixture was filtered through a celite pad and evaporated to dryness. The crude compound was dissolved in a 1:1 mixture of THF and water (150 mL). FmocOSu (2.3 g, 6.8 mmol) and K₂CO₃ (1.7 g, 12.2 mmol) were added.

The solution was allowed to react at rt overnight. After confirming the completion of the reaction by TLC, THF was evaporated. The resulting aqueous solution was acidified to pH = 2 by dropwise addition of 1M hydrochloric acid at 0 °C. The product was extracted with AcOEt, dried over MgSO₄, filtered, and concentrated *in vacuo*. The crude compound was purified by flash chromatography (Cy/AcOEt/AcOH 100:0:1 → 75:25:1) to afford a white powder (2.5 g, 72% yield); **R_f** (Cy/AcOEt/AcOH, 7:3:0.1) = 0.27; ¹H NMR (250 MHz, CDCl₃) δ 7.75 (d, *J* = 7.2 Hz, 2H, CH Ar), 7.58 (d, *J* = 7.2 Hz, 2H, CH Ar), 7.19–7.39 (m, 4H, CH Ar), 5.54 (bs, 1H, NH Fmoc), 4.95 (bs, 2H, NH Boc), 4.40 (d, *J* = 6.5 Hz, 2H, CH₂ Fmoc), 4.20 (t, *J* = 6.5 Hz, 1H, CH Fmoc), 3.38–3.41 (m, 2H, CH₂βε), 3.07 (m, 4H, CH₂δ), 1.20–1.67 (m, 26H, CH₂β, CH₂γ and C(CH₃)₃); ¹³C NMR (62.5 MHz, CDCl₃) δ 176.5 (C, C=O acid), 157.20, 156.4 (3C, C=O carbamate), 143.9, 141.3 (4C, C Ar), 129.1, 128.2, 127.7, 127.1, 125.3, 125.1, 120.0 (8CH, CH Ar), 79.3 (2C, C(CH₃)₃), 67.0 (CH₂, CH₂ Fmoc), 49.8 (CH₂, CH₂βε), 47.2 (CH, CH Fmoc), 40.7 (2CH₂, CH₂δ), 40.6 (C, Cα), 30.6 (2CH₂, CH₂β), 28.4 (6CH₃, C(CH₃)₃), 24.3 (2CH₂, CH₂γ); HRMS-ESI+: calcd for C₃₄H₄₇N₃O₈ 625.3255, calcd for C₃₄H₄₇N₃O₈Na 648.3153, found 648.3261 [M + Na]⁺.



Scheme 5. Synthesis of H-β^{2,2} h bis-Orn(Boc)₂OMe **1** and Fmoc β^{2,2} h bis-Orn(Boc)₂OH **2**.

4.3.2. Synthesis of Boc-β^{3,3} h bis-Orn(Boc)₂OH **3** (Scheme 6)

1-Benzyl 3-tert-butyl 2,2-bis(2-cyanoethyl)malonate 24: Benzyl *tert*-butylmalonate (25 g, 96.4 mmol) was mixed with acrylonitrile (14 mL, 210 mmol). Triethylamine (5.3 mL, 40 mmol) was added dropwise, followed by lithium perchlorate (5.4 g, 50 mmol). The reaction was stirred continuously and allowed to react overnight. After confirming completion of the reaction by TLC, AcOEt was added to the reaction mixture. The organic layer was washed with 5% citric acid solution and brine, dried over MgSO₄, filtered, and evaporated. The crude compound was purified by flash chromatography (Cy/AcOEt, 100:0 to 8:2) to afford a yellow oil (30.2 g, 88% yield); **R_f** (Cy/AcOEt, 8:2) = 0.37; ¹H NMR (250 MHz, CDCl₃) δ 7.37 (m, 5H, CH Ar), 5.20 (s, 2H, CH₂Ph), 2.17–2.43 (m, 8H, CH₂βαγδCH₂γ), 1.35 (s, 9H, C(CH₃)₃); ¹³C NMR (62.5 MHz, CDCl₃) δ 169.2, 167.9 (2C, C=O), 134.5 (C, C Ar), 128.9, 128.8, 128.5, 127, 126.2 (5CH, CH Ar), 118.5 (2C, C≡N), 84 (C, C(CH₃)₃), 67.9 (CH₂, CH₂Ph), 56.2 (C, Cα), 29.5 (2CH₂, CH₂β), 27.6 (3CH₃, C(CH₃)₃), 13 (2CH₂, CH₂γ); HRMS-ESI+: calcd for C₂₀H₂₄N₂O₄ 356.1736, calcd for C₂₀H₂₄N₂O₄Na 379.1634, found 379.1628 [M + Na]⁺.

2-(Tert-butoxycarbonyl)-4-cyano-2-(2-cyanoethyl)butanoic acid 5: Compound **24** (18 g, 51 mmol) was dissolved in MeOH (500 mL). Ammonium formate (16.7 g, 265 mmol) and Pd/C (5.1 g, 100 mg/mmol) were added and the reaction mixture was stirred for 3 h. Afterward, the reaction mixture was filtered through a celite pad to remove the Pd/C before evaporation to dryness. The product was diluted with dichloromethane. The organic layer was washed with 10% citric acid solution and brine, dried over MgSO₄, filtered, and evaporated to afford an oil. The product was used in the following step without further purification. (11.34 g, 83% yield); **R_f** (Cy/AcOEt/AcOH, 8:2:0.1) = 0.1; ¹H NMR (250 MHz, CDCl₃) δ 2.41–2.54 (m, 4H, CH₂β), 2.20 (t, *J* = 7.5 Hz, 4H, CH₂γ), 1.51 (s, 9H, C(CH₃)₃); ¹³C NMR

(62.5 MHz, CDCl₃) δ 173.1 (C, C=O acid), 168.3 (C, C=O ester), 118.5 (2C, C \equiv N), 84.8 (C, C(CH₃)₃), 56.2 (C, C α), 30.0 (2CH₂, CH₂ β), 27.8 (3CH₃, C(CH₃)₃), 13.1 (2CH₂, CH₂ γ); HRMS-ESI+: calcd for C₁₃H₁₈N₂O₄ 266.1267, calcd for C₁₃H₁₈N₂O₄Na 289,1165, found 289.1159 [M + Na]⁺.

1-Tert-butyl 4-methyl 2,2-bis(2-cyanoethyl)succinate 6: Compound 5 (9.0 g, 34 mmol) was dissolved in DCM under Argon. 1-Chloro-*N,N*-2-trimethylpropenylamine (9.0 mL, 68 mmol) was added. The solution was stirred for 2 h then concentrated *in vacuo*. The residue was dissolved in dry acetonitrile (170 mL) and cooled to 0 °C. DIEA (11.9 mL, 68 mmol) and a 2M solution of trimethylsilyldiazomethane in Et₂O (34 mL, 68 mmol) was added. The reaction mixture was stirred at 0 °C for 16 h. The organic solvents were evaporated *in vacuo*. The residue was dissolved in AcOEt and washed with 10% citric acid, saturated NaHCO₃ and brine. Finally, the organic layer was dried over MgSO₄, filtered, and evaporated to dryness. The crude compound was dissolved in DMF (180 mL) and MeOH (90 mL) then Ag₂O (39.4 g, 170 mmol) was added. The reaction mixture was refluxed for 10 min. After evaporation of MeOH, diethyl ether and a saturated solution of NH₄Cl were added slowly and the mixture was filtered through a celite pad. The organic layer was separated and washed with a saturated solution of NH₄Cl, dried over MgSO₄, filtered, and evaporated. The crude compound was purified by flash chromatography (Cy/AcOEt, 100:0 to 60:40) to afford a yellow oil (2.1 g, 21% yield); **R_f** (Cy/AcOEt, 1:1) = 0.6; ¹H NMR (300 MHz, CDCl₃) δ 3.71 (s, 3H, CO₂CH₃), 2.61 (s, 2H, CH₂ α), 2.27–2.37 (m, 4H, CH₂ γ), 1.91–2.07 (m, 4H, CH₂ δ), 1.48 (s, 9H, C(CH₃)₃); ¹³C NMR (75 MHz, CDCl₃) δ 171.4, 170.1 (2C, C=O), 118.8 (2C, C \equiv N), 82.5 (C, C(CH₃)₃), 51.6 (CH₃, CO₂CH₃), 46.6 (CH₂, CH₂ α), 37.4 (C, C β), 30.6 (2CH₂, CH₂ γ), 27.5 (3CH₃, C(CH₃)₃), 12.3 (2CH₂, CH₂ δ); HRMS-ESI+: calcd for C₁₅H₂₂N₂O₄ 294.1580, calcd for C₁₅H₂₂N₂O₄Na 317,1478, found 317.4718 [M + Na]⁺.

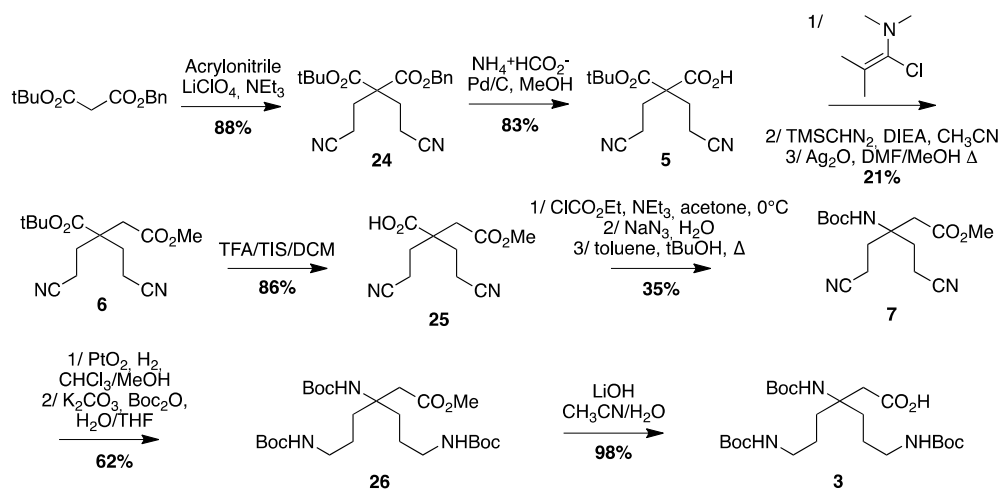
2,2-Bis(2-cyanoethyl)-4-methoxy-4-oxobutanoic acid 25: Compound 6 (1.3 g, 4.4 mmol) was dissolved in DCM (40 mL). Triisopropylsilane (900 μ L, 4.4 mmol) and TFA (40 mL) were added. The reaction mixture was stirred for 1 hour before evaporation to dryness. The crude compound was purified by flash chromatography (Cy/AcOEt/AcOH, 100:0:1 to 50:50:1) to afford a colorless oil (900 mg, 86% yield); **R_f** (Cy/AcOEt/AcOH, 5:5:0.1) = 0.34; ¹H NMR (300 MHz, CDCl₃) δ 3.66 (s, 3H, CO₂CH₃), 2.65 (s, 2H, CH₂ α), 2.30–2.49 (m, 4H, CH₂ γ), 1.98–2.16 (m, 4H, CH₂ δ); ¹³C NMR (75 MHz, CDCl₃) δ 177.9 (C, C=O acid), 170.5 (C, C=O ester), 118.7 (2C, C \equiv N), 52.4 (CH₃, CO₂CH₃), 46.3 (C, C β), 37.0 (CH₂, CH₂ α), 30.8 (2CH₂, CH₂ γ), 12.8 (2CH₂, CH₂ δ); HRMS-ESI+: calcd for C₁₁H₁₄N₂O₄ 238.0954, calcd for C₁₁H₁₄N₂O₄Na 261,0852, found 261.0845 [M + Na]⁺.

Methyl 3-((tert-butoxycarbonyl)amino)-5-cyano-3-(2-cyanoethyl)pentanoate 7: Compound 25 (450 mg, 1.9 mmol) was dissolved in dry acetone (15 mL) and cooled to 0° C. NEt₃ (300 μ L, 2.3 mmol) and ClCO₂Et (200 μ L, 2.1 mmol) were added. The reaction mixture was stirred for 1.5 h. A solution of NaN₃ (309 mg, 4.75 mmol) in H₂O (8.5 mL) was added and the mixture was stirred at 0 °C for 2 additional hours. Acetone was evaporated and the compound was extracted with toluene. The organic layer was dried over MgSO₄ and filtered. The volume was reduced by evaporation to 20 mL. *tert*-BuOH (15 mL) was added and the reaction was refluxed for 16 h. The solvent was evaporated and the crude compound purified by flash chromatography (Cy/AcOEt, 100:0 to 7:3) to afford a white powder (200 mg, 35% yield); **R_f** (Cy/AcOEt, 1:1) = 0.44; ¹H NMR (300 MHz, CDCl₃) δ 5.17 (bs, 1H, NHBoc), 3.71 (s, 3H, CO₂CH₃), 2.60 (s, 2H, CH₂ α), 2.22–2.45 (m, 6H, CH₂ γ and CH₂ δ ₁), 1.99–2.12 (m, 2H, CH₂ δ ₂), 1.40 (s, 9H, C(CH₃)₃); ¹³C NMR (75 MHz, CDCl₃) δ 170.4 (C, C=O ester), 154.3 (C, C=O carbamate), 119.2 (2C, C \equiv N), 80.5 and 80.4 (2C, C(CH₃)₃), 55.3 (C, C β), 52.4 (CH₃, CO₂CH₃), 39.5 (CH₂, CH₂ α), 31.8 (2CH₂, CH₂ γ), 28.3 (3CH₃, C(CH₃)₃), 12.0 (2CH₂, CH₂ δ); HRMS-ESI+: calcd for C₁₅H₂₃N₃O₄ 309.1689, calcd for C₁₅H₂₃N₃O₄Na 332,1587, found 332.1581 [M + Na]⁺.

Methyl-3,6-bis((tert-butoxycarbonyl)amino)-3-(3-((tert-butoxycarbonyl)amino)propyl) hexanoate 26: Compound 7 (145 mg, 0.47 mmol) was dissolved in a 9:1 mixture of methanol and chloroform. PtO₂ (16 mg, 0.07 mmol) was added and the reaction mixture was stirred under 5 bars of H₂ pressure at rt for 3 days. The reaction mixture was filtered through a celite pad and evaporated to dryness. The crude

product was dissolved in a 1:1 mixture of THF/H₂O and Boc₂O was added. After stirring overnight, THF was evaporated and the product was extracted with DCM. The organic layer was washed with brine, dried over MgSO₄, filtered, and evaporated *in vacuo*. The crude compound was purified by flash chromatography (Cy/AcOEt, 7:3) to afford a colorless oil (150 mg, 62% yield); **R_f** (Cy/AcOEt, 1:1) = 0.68; ¹H NMR (300 MHz, CDCl₃) δ 4.85 (bs, 1H, NH Boc), 4.72 (bs, 2H, NH Boc), 3.64 (s, 3H, CO₂CH₃), 3.02–3.11 (m, 4H, CH₂ε), 2.61 (s, 2H, CH₂α), 1.56–1.77 (m, 4H, CH₂γ), 1.34–1.48 (m, 31H, CH₂δ and C(CH₃)₃); ¹³C NMR (75 MHz, CDCl₃) δ 171.7 (C, C=O ester), 156.0 (2C, C=O carbamate), 154.5 (C, C=O carbamate), 79.1 (3C, C(CH₃)₃), 56.1 (C, Cβ), 51.6 (CH₃, CO₂CH₃), 40.5 (2CH₂, CH₂ε), 40.3 (CH₂, CH₂α), 33.3 (2CH₂, CH₂β), 28.4 (9CH₃, C(CH₃)₃), 23.8 (2CH₂, CH₂γ); HRMS-ESI⁺: calcd for C₂₅H₄₇N₃O₈ 517.3363, calcd for C₂₅H₄₇N₃O₈Na 540.3261, found 540.3255 [M + Na]⁺.

Boc-β^{3,3} hbis-Orn(Boc)₂OH 3: Compound **26** (0.130 g, 0.25 mmol) was dissolved in a 1:1 mixture of THF/H₂O. LiOH (12 mg, 0.5 mmol) was added and the reaction mixture was stirred at rt for 5 days. THF was evaporated and the resulting aqueous solution was acidified to pH = 2 by dropwise addition of 1 M hydrochloric acid at 0 °C. The product was extracted with DCM and the organic layer was washed with brine, dried over MgSO₄, filtered, and evaporated to afford a white powder (120 mg, 98% yield). The product was used in following step without any further purification; **R_f** (Cy/AcOEt, 1:1) = 0.20; ¹H NMR (300 MHz, MeOD) δ 3.01 (t, *J* = 6.6 Hz, 4H, CH₂ε), 2.62 (s, 2H, CH₂α), 1.73 (m, 4H, CH₂γ), 1.42 (m, 31H, CH₂δ and C(CH₃)₃); ¹³C NMR (75 MHz, MeOD) δ 158.6 (3C, C=O carbamate), 80.0 (3C, C(CH₃)₃), 57.2 (C, Cβ), 41.7 (3CH₂, CH₂α and CH₂ε), 34.3 (2CH₂, CH₂γ), 29.0 (9CH₃, C(CH₃)₃), 25.0 (2CH₂, CH₂δ); HRMS-ESI⁺: calcd for C₂₄H₄₅N₃O₈ 503.3207, calcd for C₂₄H₄₅N₃O₈Na 526.3105, found 526.3099 [M + Na]⁺; IR (ATR) ν (cm⁻¹): 3346.9 (-OH acid), 2962.3, 2975.8, 2872.9, 2495.0, 1686.5 (C=O acid), 1514.6, 1479.5, 1453.5, 1392.0, 1365.3, 1273.7, 1248.7, 1162.3, 1092.6, 985.2, 866.5, 778.8.

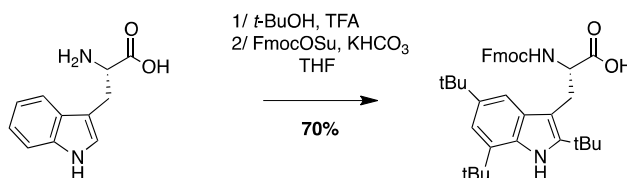


Scheme 6. Synthesis of Boc-β^{3,3} hbis-Orn(Boc)₂OH **3**.

4.3.3. Synthesis of Fmoc-Tbt-OH (Scheme 7)

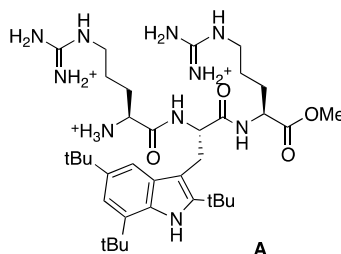
(S)-2-(((9H-Fluoren-9-yl)methoxy)carbonyl)amino)-3-(2,4,6-tri-tert-butyl-1H-indol-3-yl) propanoic Acid: A mixture of H-Trp-OH (3 g, 14.6 mmol) and *tert*-BuOH (31 mL, 323 mmol) in TFA (90 mL) was stirred at rt for 20 days. The resulting dark solution was evaporated to dryness to give a black oil, and water (50 mL) was added. To the resulting suspension was added KHCO₃ until pH = 8–9. THF (50 mL) and FmocOSu (5.4 g, 16.0 mmol) were added and the mixture was stirred for 16 h. THF was evaporated and the solution was acidified to pH = 2. The compound was extracted with AcOEt, dried over MgSO₄, filtered, and concentrated *in vacuo*. The crude compound was purified by flash chromatography (Cy/AcOEt/AcOH 100:0:1 to 50:50:1) to afford a white powder (6 g, 70% yield); **R_f** (Cy/AcOEt/AcOH, 5:5:0.1) = 0.66; ¹H NMR (300 MHz, CDCl₃) δ 7.12–8.08 (m, 10H, CH Ar), 4.65–4.88 (m, 1H, CH Fmoc), 4.22–4.43 (m, 2H, CH₂ Fmoc), 4.17 (t, *J* = 6.8 Hz, 1H, CHα), 3.56–3.74 (m, 1H, CH₂β₁), 3.42 (dd, *J* =

14.8 Hz, 9.1 Hz, 1H, $CH_2\beta_2$), 1.57 (s, 18H, $C(CH_3)_3$), 1.45 (s, 9H, $C(CH_3)_3$); ^{13}C NMR (75 MHz, $CDCl_3$) δ 177.7 (C, C=O acid), 156.1 (C, C=O carbamate), 143.8, 143.7, 142.9, 142.7, 141.2, 132.0, 130.2, 129.8 (9C, C Ar), 127.6, 127.0, 125.2, 125.1, 119.8, 116.9, 111.6 (10C, CH Ar), 103.9 (C, C Ar), 67.2 (CH_2 , CH_2 Fmoc), 55.3 (CH, $CH\alpha$), 47.0 (CH, CH Fmoc), 34.8 (2C, $C(CH_3)_3$), 33.1 (C, $C(CH_3)_3$), 32.0, 30.9, 30.6 (9 CH_3 , $C(CH_3)_3$), 27.6 (CH_2 , $CH_2\beta$); HRMS-ESI+: calcd for $C_{38}H_{46}N_2O_4$ 594.3458, calcd for $C_{38}H_{46}N_2O_4Na$ 617.3356, found 617.3350 $[M + Na]^+$.



Scheme 7. Synthesis of Fmoc-Tbt-OH.

4.3.4. Synthesis of Peptide A: Arg-Tbt-Arg-NH₂

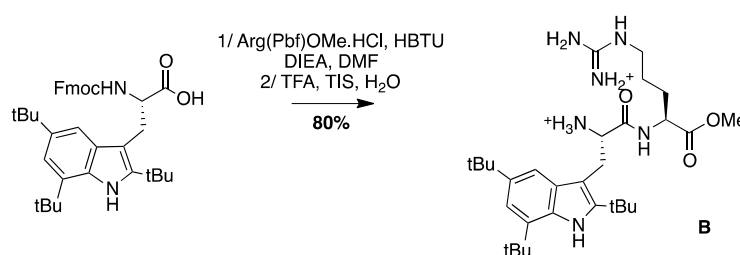


Fmoc Rink Amide resin loaded at 0.43 mmol/g (162 mg, 0.07 mmol) was washed with DMF and allowed to swell in DMF for 15 min. Fmoc deprotection was achieved through treatment of the resin with a solution of 20% piperidine (*v:v*) in DMF (5 min, 3 times), followed by washing with NMP. Fmoc-Arg(Pbf)-OH (4 eq, 0.28 mmol, 182 mg) was dissolved in dry NMP and HATU (3.6 eq, 0.25 mmol, 95 mg) and DIEA (10 eq, 0.7 mmol, 130 μ L) were added. The resulting solution was added to the resin and the mixture was stirred for 2 h then filtrated and washed with NMP. Removal of the Fmoc protecting group was achieved by treatment of the resin with 20% (*v:v*) piperidine in DMF (3 times for 5 min). The resin was washed with NMP. Fmoc-Tbt-OH (4 eq, 0.28 mmol, 166 mg) was dissolved in NMP (1.5 mL). HATU (3.6 eq, 0.25 mmol, 95 mg) and DIEA (10 eq, 0.7 mmol, 130 μ L) were added. The solution was added to the resin and the coupling reaction was allowed to proceed for 1.5 h at room temperature. The solution was removed by filtration and the resin was washed with DMF. After removal of the Fmoc protective group (20% piperidine in DMF, 5 min, 3 times) and washing of the resin with NMP, a solution of Fmoc-Arg(Pbf)-OH (4 eq, 0.28 mmol, 182 mg), HATU (3.6 eq, 0.25 mmol, 95 mg), and DIEA (10 eq, 0.7 mmol, 130 μ L) in NMP (2 mL) was added and the reaction mixture was stirred for 2 h then filtrated and washed with NMP. Simultaneous final deprotection and cleavage from the resin was achieved by treating the resin with a TFA/TIS/H₂O cocktail (95:2.5:2.5, 3 mL) for 4 h. The crude peptide was precipitated through addition of cold diethyl ether. Purification by preparative RP-HPLC using a gradient of 15% to 90% MeCN in 30 min gives after lyophilisation peptide A as a white powder with a purity of >95%. MALDI-TOF: calcd for $C_{36}H_{62}N_{10}O_3$ 683, found 684.4 $[M + H]^+$, 706.4 $[M + Na]^+$, 722.4 $[M + K]^+$; HPLC (Water/ACN (0.1% TFA); 15% to 100% ACN in 30 min): *tr* = 10.19 min.

4.3.5. Synthesis of Peptide B, Tbt-Arg-OMe B (Scheme 8)

Boc-Tbt-OH (50 mg, 0.11 mmol) was dissolved in DMF. HBTU (42 mg, 0.11 mmol) and DIEA (40 μ L, 0.22 mmol) were added and the mixture was stirred for 5 min before addition of H-Arg(Pbf)OMe (52 mg, 0.11 mmol). The reaction mixture was stirred at room temperature for 5 h, then diluted with Et₂O and washed with an aqueous saturated solution of NH₄Cl. The organic layer was dried over MgSO₄,

filtered, and evaporated to dryness. The crude compound was purified by flash chromatography (Cy/AcOEt, 100:0 to 50:50) to afford the pure protected dipeptide as a white powder (80 mg, 80% yield). Treatment of this compound with a cocktail of TFA/TIS/H₂O (95:2.5:2.5) for 4 h, followed by evaporation to dryness lead to peptide **B**, which was purified by preparative RP-HPLC using a gradient of 30% to 50% MeCN in 30 min. After lyophilisation, peptide **B** was obtained as white powder with purity >98%; ¹H NMR (300 MHz, MeOD) δ 7.24 (s, 1H, CH indole), 7.11 (s, 1H, CH indole), 4.25 (t, J = 6, 1H, CH α Arg), 4.08 (t, J = 8.1, 1H, CH α Tbt), 3.42 (d, J = 8.1, 1H, CH₂ β Tbt), 3.39 (s, 3H, COOCH₃), 3.09–3.15 (m, 2H, CH₂ δ Arg), 1.70–1.74 (m, 1H, CH₂ γ_1 Arg), 1.44–1.57 (m, 3H, CH₂ γ_2 and CH₂ β Arg), 1.54 (s, 9H, C(CH₃)₃), 1.50 (s, 9H, C(CH₃)₃), 1.37 (s, 9H, C(CH₃)₃); MALDI-TOF: calcd for C₃₀H₅₀N₆O₃ 542.4, found 543.2 [M + H]⁺, 565.2 [M + Na]⁺; HPLC (Water/ACN (0.1% TFA); 5% to 100% ACN in 30 min: tr = 15.15 min.



Scheme 8. Synthesis of Peptide B, Tbt-Arg-OMe B.

4.3.6. Synthesis of Peptides 8–12 by LPPS (Scheme 9)

Synthesis of Trp- $\beta^{2,2}$ h bis-Orn-OMe **8** and Gdm-Trp- $\beta^{2,2}$ h bis-Arg-OMe **10**

Boc Trp- $\beta^{2,2}$ h bis-Orn(Boc)₂-OMe 15: Boc-Tbt-OH (60 mg, 0.2 mmol) was dissolved in DMF (6 mL). HBTU (76 mg, 0.2 mmol) and DIEA (80 μ L, 0.4 mmol) were added and the mixture was stirred for 5 min before addition of H- $\beta^{2,2}$ h bis-Orn(Boc)₂OMe **1** (84 mg, 0.2 mmol). The reaction mixture was stirred at room temperature overnight, then diluted with Et₂O and washed with an aqueous saturated solution of NH₄Cl. The organic layer was dried over MgSO₄, filtered, and evaporated to dryness. The crude compound was purified by flash chromatography (Cy/AcOEt, 70:30) to afford **15** as a white powder (140 mg, 99% yield). ¹H NMR (300 MHz, MeOD) δ 7.71 (d, J = 7.8, 1H, CH Ar), 7.38 (d, J = 7.2, 1H, CH Ar), 7.19 (td, J = 7.2, 1.1, 1H, CH Ar), 7.13 (td, J = 7.8, 1.1, 1H, CH Ar), 7.06 (d, J = 2.1, 1H, CH Ar), 5.91 (br, 1H, NH Boc), 5.36 (br, 1H, NH Boc), 4.78 (br, 1H, CH α Trp), 4.72 (br, 1H, CH₂ β_1 Trp), 4.52 (br, 1H, CH₂ β_2 Trp), 3.66 (s, 3H, CO₂CH₃), 3.30–3.35 (m, 2H, CH₂ β_{ϵ_1} $\beta^{2,2}$ h bis-Orn), 3.09–3.23 (m, 2H, CH₂ β_{ϵ_2} $\beta^{2,2}$ h bis-Orn), 2.95–3.04 (m, 4H, CH₂ δ $\beta^{2,2}$ h bis-Orn), 1.52 (s, 27H, C(CH₃)₃), 1.42–1.15 (m, 8H, CH₂ $\beta_{\alpha\gamma\delta}$ $\beta^{2,2}$ h bis-Orn).

Trp- $\beta^{2,2}$ h bis-Orn-OMe 8: Compound **15** (70 mg, 0.1 mmol) was dissolved in DCM (~0.4 M) and an equivalent volume of TFA/TIS/H₂O (95:2.5:2.5). The mixture was stirred at rt for 1 h then evaporated to dryness. The crude product was purified by preparative RP-HPLC using a gradient of 10% to 50% MeCN in 30 min. After lyophilisation compound **8** was obtained as white powder with purity >95% (30 mg, 70% yield); ¹H NMR (500 MHz, D₂O) δ 7.68 (d, J = 8, 1H, CH Ar), 7.55 (d, J = 12.8, 1H, CH Ar), 7.33 (s, 1H, CH Ar), 7.30 (t, J = 8, 1H, CH Ar), 7.22 (t, J = 7.5, 1H, CH Ar), 4.42 (dd, J = 9.5, 6, 1H, CH α Trp), 3.66 (s, 3H, CO₂CH₃), 3.51 (d, J = 14.5, 1H, CH₂ β_{ϵ_1} $\beta^{2,2}$ h bis-Arg), 3.41 (dd, J = 14.2, 6, 1H, CH₂ β_1 Trp), 3.35 (dd, J = 14.2, 9.5, 1H, CH₂ β_2 Trp), 3.15 (d, J = 14.5, 1H, CH₂ β_{ϵ_2} $\beta^{2,2}$ h bis-Arg), 2.81 (t, J = 7.8, 1H, CH₂ δ_1 $\beta^{2,2}$ h bis-Arg), 2.71 (t, J = 7.8, 1H, CH₂ δ_2 $\beta^{2,2}$ h bis-Arg), 1.49–1.53 (m, 1H, CH₂ γ_1 $\beta^{2,2}$ h bis-Arg), 1.35–1.39 (m, 3H, CH₂ γ_1 and CH₂ γ_2 $\beta^{2,2}$ h bis-Arg), 1.24 (td, J = 13.2, 3.7, 1H, CH₂ β_1 $\beta^{2,2}$ h bis-Arg), 1.05–1.12 (m, 2H, CH₂ β_1 and CH₂ β_2 $\beta^{2,2}$ h bis-Arg), 0.88–0.95 (m, 1H, CH₂ β_2 $\beta^{2,2}$ h bis-Arg); MALDI-TOF: calcd for C₂₁H₃₃N₅O₃ 403.3, calcd for C₂₁H₃₃N₅O₃Na 426.3, found 404.5 [M + H]⁺, 426.5 [M + Na]⁺, 442.5 [M + K]⁺; HPLC (Water/ACN (0.1% TFA); 5% to 100% ACN in 30 min): tr = 7.18 min (Figure 11).

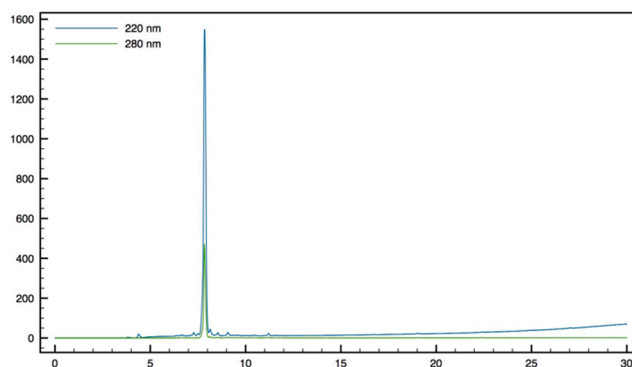


Figure 11. HPLC profile of *Trp-β^{2,2} h bis-Orn-OMe 8*.

Gdm-Trp-β^{2,2} h bis-Arg-OMe 10: Compound **15** (70 mg, 0.1 mmol) was dissolved in DCM (~0.4 M) and an equivalent volume of TFA/TIS/H₂O (95:2.5:2.5). The mixture was stirred at rt for 1.5 h then evaporated to dryness. The crude compound was dissolved in 6 mL of THF. 1,3-Di-Boc-2-(trifluoromethylsulfonyl)guanidine (137 mg, 0.35 mmol) and NEt₃ (60 μL, 0.4 mmol) were added and the reaction mixture was stirred at rt overnight. After evaporation of THF, a solution of TFA/TIS/H₂O (95:2.5:2.5) was added and the mixture was stirred at rt for 2 h. The crude product was purified by preparative RP-HPLC using a gradient of 10% to 50% MeCN in 30 min. After lyophilisation, compound **10** was obtained as white powder with purity >98% (31 mg, 57% yield); ¹H NMR (300 MHz, D₂O) δ 7.69 (d, *J* = 7.5, 1H, CH Ar), 7.36 (d, *J* = 8.1, 1H, CH Ar), 7.31 (s, 1H, CH Ar), 7.26 (td, *J* = 7.5, 0.9, 1H, CH Ar), 7.22 (td, *J* = 7.2, 0.9, 1H, CH Ar), 4.62 (t, *J* = 7.5, 1H, CH α Trp), 3.69 (s, 3H, CO₂CH₃), 3.47 (d, *J* = 14.1, 1H, CH₂ β ϵ ₁ $\beta^{2,2}$ h bis-Arg), 3.35 (d, *J* = 7.5, 2H, CH₂ β Trp), 3.21 (d, *J* = 14.4, 1H, CH₂ β ϵ ₂ $\beta^{2,2}$ h bis-Arg), 3.05 (t, *J* = 6.6, 1H, CH₂ δ ₁ $\beta^{2,2}$ h bis-Arg), 2.98 (dd, *J* = 11.7, 6.6, 1H, CH₂ δ ₂ $\beta^{2,2}$ h bis-Arg), 1.29–1.43 (m, 4H, CH₂ γ $\beta^{2,2}$ h bis-Arg), 1.09–1.28 (m, 4H, CH₂ β $\beta^{2,2}$ h bis-Arg); MALDI-TOF: calcd for C₃₂H₅₇N₅O₃ 529.3, calcd for C₃₂H₅₇N₅O₃Na 552.3, found 530.6 [M + H]⁺, 552.6 [M + Na]⁺, 513.6 [M + H – NH₃]⁺; HPLC (Water/ACN (0.1% TFA); 5% to 100% ACN in 30 min): tr = 9.62 min (Figure 12).

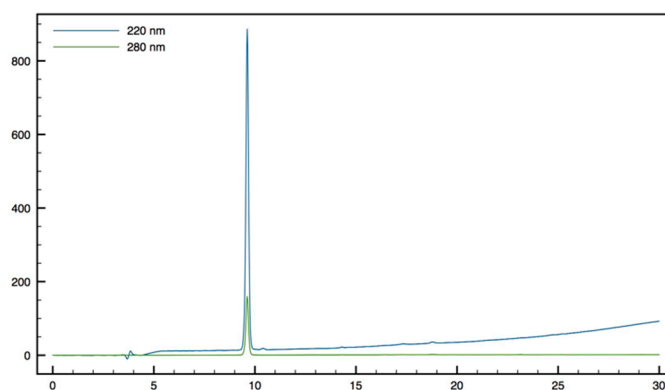


Figure 12. HPLC profile of *Gdm-Trp-β^{2,2} h bis-Arg-OMe 10*.

Synthesis of *Tbt-β^{2,2} h bis-Orn-OMe 9*, *Tbt-β^{2,2} h bis-Arg-OMe 11* and *Gua-Tbt-β^{2,2} h bis-Arg-OMe 12*

Fmoc-Tbt-β^{2,2} h bis-Orn(Boc)₂OMe 16: Fmoc-Tbt-OH (400 mg, 0.64 mmol) was dissolved in DMF (24 mL). HBTU (244 mg, 0.64 mmol) and DIEA (240 μL, 1.28 mmol) were added and the mixture was stirred for 3 h before addition of H-β^{2,2} h bis-Orn(Boc)₂OMe **1** (268 mg, 0.64 mmol). The reaction mixture was stirred at room temperature overnight, then diluted with Et₂O and washed with an aqueous saturated solution of NH₄Cl. The organic layer was dried over MgSO₄, filtered, and evaporated to dryness. The crude compound was purified by flash chromatography (Cy/AcOEt, 100:0 to 70:30) to afford the pure protected dipeptide as a white powder (450 mg, 70% yield). ¹H NMR (300 MHz, MeOD) δ 8.22 (s,

1H, NH indole), 7.75 (d, $J = 7.2$, 1H, CH Ar Fmoc), 7.55 (d, $J = 7.2$, 1H, CH Ar Fmoc), 7.41 (s, 1H, CH Ar indole), 7.35 (t, $J = 7.2$, 1H, CH Ar Fmoc), 7.24 (dt, $J = 11.7$ and 7.2 , 1H, CH Ar Fmoc), 7.12 (s, 1H, CH indole), 4.27–4.33 (m, 3H, CH α Tbt and CH $_2$ Fmoc), 4.12 (t, $J = 6.9$, 1H, CH Fmoc), 3.55 (s, 3H, CO $_2$ CH $_3$), 3.43 (dd, $J = 14.1$ 9.3, 1H, CH $_2\beta_1$ Tbt), 3.39 (d, $J = 14.1$, 1H, CH $_2\beta_{\epsilon_1}$ $\beta^{2,2}$ *h* bis-Orn), 3.23 (dd, $J = 14.4$, 6.3, 1H, CH $_2\beta_2$ Tbt), 2.9 (m, 4H, CH $_2\delta$ $\beta^{2,2}$ *h* bis-Orn), 2.79 (d, $J = 14.1$, 1H, CH $_2\beta_{\epsilon_2}$ $\beta^{2,2}$ *h* bis-Orn), 1.52 (s, 9H, C(CH $_3$) $_3$ indole), 1.47 (s, 9H, C(CH $_3$) $_3$ indole), 1.36–1.44 (m, 35H, C(CH $_3$) $_3$ indole, C(CH $_3$) $_3$ Boc, CH $_2\beta$ $\beta^{2,2}$ *h* bis-Orn and CH $_2\gamma$ $\beta^{2,2}$ *h* bis-Orn); 13 C NMR (75 MHz, MeOD) δ 177.1 (C, C=O amide), 174.9 (C, C=O ester), 158.4 (C=O Boc), 157.9 (C=O Fmoc), 145.2, 145.1, 143.6, 142.9, 142.5, 133.1, 131.8, 131.3 (8C, C Ar), 128.7, 128.2, 126.2, 120.9 (4CH, CH Ar Fmoc), 117.3, 113.4 (2CH, CH Ar indole), 106.2 (C, C Ar), 79.8 (C, C(CH $_3$) $_3$ Boc), 68.1 (CH $_2$, CH $_2$ Fmoc), 58.5 (CH, CH α Tbt), 52.3 (CH $_3$, CO $_2$ CH $_3$), 50.7 (C, C α $\beta^{2,2}$ *h* bis-Orn), 48.3 (CH, CH Fmoc), 42.9 (CH $_2$, CH $_2\beta_{\epsilon}$ $\beta^{2,2}$ *h* bis-Orn), 41.6 (CH $_2$, CH $_2\delta$ $\beta^{2,2}$ *h* bis-Orn), 35.7, 35.5 and 34.3 (3C, C(CH $_3$) $_3$ indole), 32.7 (CH $_3$, C(CH $_3$) $_3$ indole), 32.4 and 32.1 (CH $_2$, CH $_2\gamma$ $\beta^{2,2}$ *h* bis-Orn), 31.3 (CH $_3$, C(CH $_3$) $_3$ indole), 30.9 (CH $_3$, C(CH $_3$) $_3$ indole), 29 (CH $_2$, CH $_2\beta$ Tbt), 28.8 (6CH $_3$, C(CH $_3$) $_3$ Boc), 25.5 and 25.3 (CH $_2$, CH $_2\beta$ $\beta^{2,2}$ *h* bis-Orn).

H-Tbt- $\beta^{2,2}$ *h* bis-OrnOMe **9**: Compound **16** (60 mg, 0.06 mmol) was dissolved in a 20% solution of piperidine in DCM and allowed to react for 1 h before evaporation to dryness. A solution of TFA/TIS/H $_2$ O (95:2.5:2.5) was added and the mixture was stirred at rt for 1 h. The crude product was purified by preparative RP-HPLC using a gradient of 30% to 50% MeCN in 30 min. After lyophilisation **9** was obtained as white powder with a purity of 98% (20 mg, 58% yield); 1 H NMR (300 MHz, D $_2$ O) δ 8.54 (s, 1H, NH indole), 7.26 (s, 1H, CH Ar), 7.22 (s, 1H, CH Ar), 4.03 (dd, $J = 9.3$, 6, 1H, CH α Tbt), 3.50 (s, 3H, CO $_2$ CH $_3$), 3.37 (d, $J = 14.2$, 1H, CH $_2\beta_{\epsilon_1}$ $\beta^{2,2}$ *h* bis-Orn), 3.34 (d, $J = 14.1$, 2H, CH $_2\beta$ Tbt), 2.80 (m, 4H, CH $_2\delta$ $\beta^{2,2}$ *h* bis-Orn), 2.33 (d, $J = 14.2$, 1H, CH $_2\beta_{\epsilon_2}$ $\beta^{2,2}$ *h* bis-Orn), 1.31–1.44 (m, 35H, CH $_2\beta$ $\beta^{2,2}$ *h* bis-Orn, CH $_2\gamma$ $\beta^{2,2}$ *h* bis-Orn and C(CH $_3$) $_3$); MALDI-TOF: calcd for C $_{32}$ H $_{57}$ N $_5$ O $_3$ 571.5, found 572.6 [M + H] $^+$; HPLC (Water/ACN (0.1% TFA); 30% to 50% ACN in 30 min): tr = 12.73 min (Figure 13).

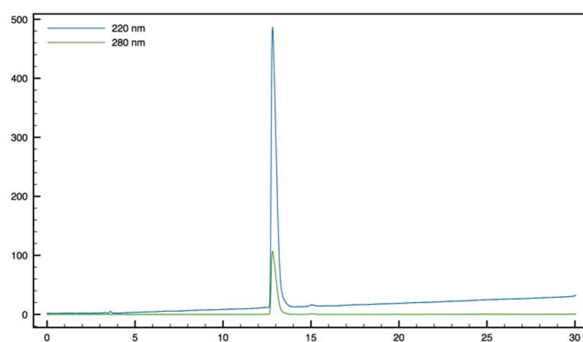


Figure 13. HPLC profile of *H*-Tbt- $\beta^{2,2}$ *h* bis-OrnOMe **9**.

H-Tbt- $\beta^{2,2}$ *h* bis-Arg-OMe **11** and *Gua*-Tbt- $\beta^{2,2}$ *h* bis-Arg-OMe **12**: Compound **9** (10 mg, 0.013 mmol) was dissolved in 1 mL of THF. 1,3-Di-Boc-2-(trifluoromethylsulfonyl) guanidine (30 mg, 0.08 mmol) and DIEA (27 μ L, 0.156 mmol) were added and the reaction mixture was stirred at rt for 2 h. After evaporation of THF, a solution of TFA/TIS/H $_2$ O (95:2.5:2.5) was added and the mixture was stirred at rt for 2 h. The crude product was evaporated *in vacuo* and purified by preparative RP-HPLC using a gradient of 30% to 50% MeCN in 30 min. Two pics were collected separately at 14 and 18 min corresponding, respectively, to compounds **11** and **12**. After lyophilisation, the two compounds **11** (5 mg, 59% yield) and **12** (2 mg, 22% yield) were obtained as white powders with purity >99%.

H-Tbt- $\beta^{2,2}$ *h* bis-Arg-OMe **11**: 1 H NMR (500 MHz, D $_2$ O) δ 7.29 (s, 1H, CH indole), 7.27 (s, 1H, CH indole), 4.14 (dd, $J = 11.2$, 5.5, 1H, CH α Tbt), 3.61 (dd, $J = 14.5$, 5, 1H, CH $_2\beta_1$ Tbt), 3.57 (s, 3H, CO $_2$ CH $_3$), 3.44 (dd, $J = 13.5$, 12, 2H, CH $_2\beta_2$ Tbt), 3.21 (d, $J = 14.5$, 1H, CH $_2\beta_{\epsilon_1}$ $\beta^{2,2}$ *h* bis-Arg), 3.04 (m, $J = 4$ H, CH $_2\delta$ $\beta^{2,2}$ *h* bis-Arg), 1.83 (d, $J = 14.5$, 1H, CH $_2\beta_{\epsilon_2}$ $\beta^{2,2}$ *h* bis-Arg), 1.55 (s, 9H, C(CH $_3$) $_3$), 1.49 (s, 9H, C(CH $_3$) $_3$), 1.39 (s, 9H, C(CH $_3$) $_3$), 1.1–1.34 (m, 8H, CH $_2\beta$ $\beta^{2,2}$ *h* bis-Arg and CH $_2\gamma$ $\beta^{2,2}$ *h* bis-Arg); MALDI-TOF:

calcd for $C_{35}H_{61}N_5O_3$ 655.5, calcd for $C_{35}H_{61}N_5O_3Na$ 678.5, found 656.4 $[M + H]^+$, 678.4 $[M + Na]^+$, 694.4 $[M + K]^+$, 639.4 $[M + H - NH_3]^+$; HPLC (Water/ACN (0.1% TFA)); 30% to 50% ACN in 30 min: $t_r = 16.11$ min (Figure 14).

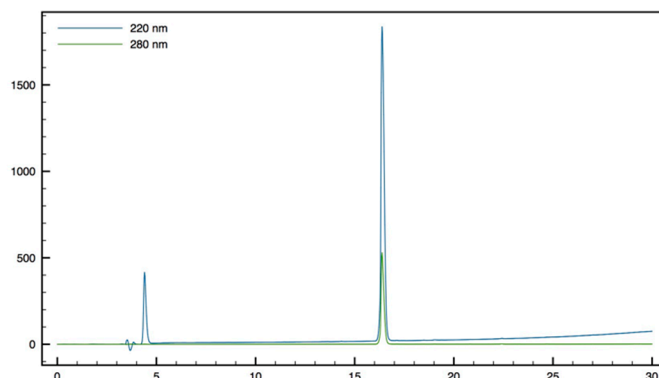


Figure 14. HPLC profile of *H-Tbt- $\beta^{2,2}$ h bis-Arg-OMe 11*.

Gua-Tbt- $\beta^{2,2}$ h bis-Arg-OMe 12: 1H NMR (300 MHz, MeOD) δ 8.35 (s, 1H, NH indole), 7.31 (d, $J = 1.5$, 1H, CH Ar), 7.14 (d, $J = 1.5$, 1H, CH Ar), 4.39 (t, $J = 7.2$, 1H, $CH\alpha$ Tbt), 3.65 (s, 3H, CO_2CH_3), 3.52 (d, $J = 14.2$, 1H, $CH_2\beta_{\epsilon_1}$ $\beta^{2,2}$ h bis-Arg), 3.47 (dd, $J = 11.1, 7.2$, 2H, $CH_2\beta$ Tbt), 3.01–3.13 (m, 4H, $CH_2\delta$ $\beta^{2,2}$ h bis-Arg), 2.82 (d, $J = 14.2$, 1H, $CH_2\beta_{\epsilon_2}$ $\beta^{2,2}$ h bis-Arg), 1.26–1.64 (m, 35H, $CH_2\beta$ $\beta^{2,2}$ h bis-Arg, $CH_2\gamma$ $\beta^{2,2}$ h bis-Arg and $C(CH_3)_3$); MALDI-TOF: calcd for $C_{36}H_{63}N_{11}O_3$ 697.5, calcd for $C_{36}H_{63}N_{11}O_3Na$ 720.5, found 698.4 $[M + H]^+$, 720.4 $[M + Na]^+$, 736.3 $[M + K]^+$, 681.3 $[M + H - NH_3]^+$; HPLC (Water/ACN (0.1% TFA)); 30% to 70% ACN in 30 min): $t_r = 14.08$ min (Figure 15).

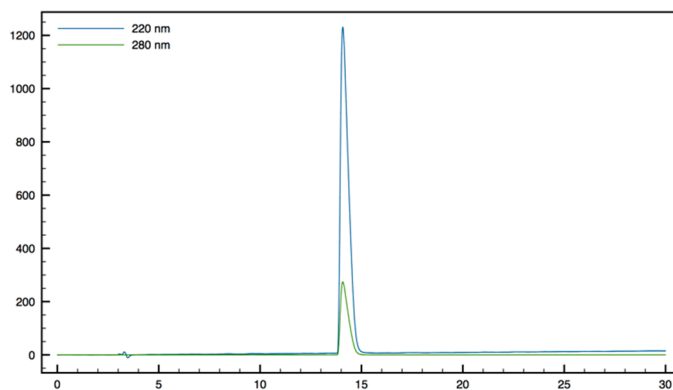
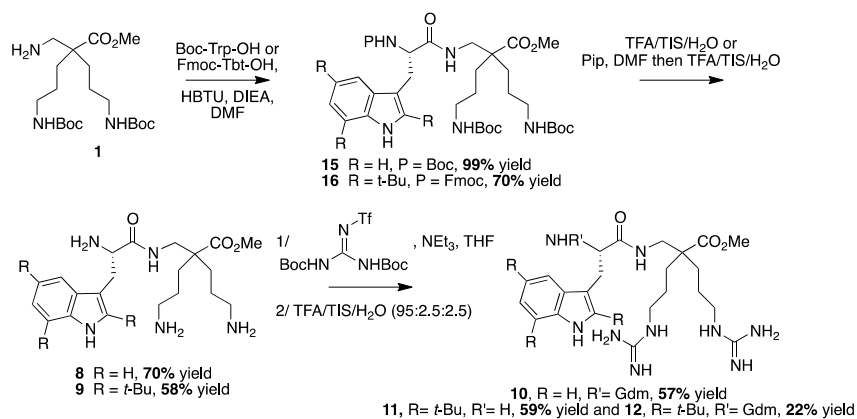


Figure 15. HPLC profile of *Gua-Tbt- $\beta^{2,2}$ h bis-Arg-OMe 12*.



Scheme 9. Synthesis of peptides 8–12 by LPPS.

4.3.7. Synthesis of Peptides 13 and 14 by SPPS (Scheme 10)

H- $\beta^{3,3}$ -*h*-bis-Arg-Tbt-OMe **13**: HMBA-AM resin (108 mg, 0.1 mmol) was washed five times with DMF, DCM, and DMF, then allowed to swell in DMF for 30 min. Fmoc-Tbt-OH (4 eq, 0.4 mmol, 238 mg) was dissolved in dry DCM. The solution was cooled to 0 °C, DIC (4 eq, 0.4 mmol, 60 μ L) was added. The reaction was stirred for 1.5 h and the solvent was then removed *in vacuo*. The resulting anhydride was dissolved in DMF and added to the resin. A solution of DMAP (0.1 eq, 0.04 mmol, 5 mg) in DMF was added and the resin was shaken for 1 h before washing with DMF, DCM, and DMF (resin loading = 0.84 mmol/g). Removal of the Fmoc protecting group was achieved by treatment of the resin with 20% (*v:v*) piperidine in DMF 3 times for 5 min. The resin was washed five times with DMF. Boc- $\beta^{3,3}$ *h* bis-Orn(Boc)₂OH **3** (2 eq, 0.18 mmol, 90 mg) was dissolved in DMF (1.2 mL). HATU (1.8 eq, 0.17 mmol, 65 mg) and DIEA (2 eq, 0.18 mmol, 23 μ L) were added. The solution was added to the resin (0.09 mmol, 108 mg) and the coupling reaction was allowed to proceed for 2 h at room temperature. The solution was removed by filtration and the resin was washed with DMF five times. Reaction completion was monitored by Kaiser test. Boc removal was performed by treating the resin with a TFA/TIS/H₂O cocktail (95:2.5:2.5) for 5 h. The free amines were then reacted with 1,3-Di-Boc-2-(trifluoromethylsulfonyl)guanidine (10 eq, 1.8 mmol, 700 mg) and NEt₃ (10 eq, 1.8 mmol, 240 μ L) in DMF overnight. The resin was filtrated and the Boc groups were removed with a TFA/TIS/H₂O cocktail (95:2.5:2.5) at rt for 3 h. After filtration, peptide **14** was cleaved from the resin using a mixture of MeOH/DMF/DIEA (5:5:1) for 16 h at 50 °C. The solution was filtrated, and solvents were evaporated. The crude product was purified by preparative RP-HPLC using a gradient of 30% to 70% MeCN in 30 min. After lyophilisation peptide **13** was obtained as a white powder with a purity of >95% (47 mg, 75% yield); ¹H NMR (500 MHz, D₂O) δ 7.37 (d, *J* = 1.7, 1H, CH Ar indole), 7.28 (d, *J* = 1.7, 1H, CH Ar indole), 4.69 (t, *J* = 7.5, 1H, CH α Tbt), 3.48–3.53 (m, 1H, CH₂ β_1 Tbt), 3.68 (dd, *J* = 10.5, 1, 1H, CH₂ β_2 Tbt), 3.25 (t, *J* = 6.5, 1H, CH₂ ϵ_1 $\beta^{2,2}$ *h* bis-Arg), 3.17 (t, *J* = 6.5, 1H CH₂ ϵ_2 $\beta^{2,2}$ *h* bis-Arg), 2.69 (d, *J* = 16, 1H, CH₂ α_1 $\beta^{2,2}$ *h* bis-Arg), 2.55 (d, *J* = 16, 1H, CH₂ α_2 $\beta^{2,2}$ *h* bis-Arg), 1.70–1.75 (m, 4H, CH₂ γ $\beta^{2,2}$ *h* bis-Arg), 1.64–1.68 (m, 2H, CH₂ δ_1 $\beta^{2,2}$ *h* bis-Arg), 1.55–1.61 (m, 2H, CH₂ δ_2 $\beta^{2,2}$ *h* bis-Arg), 1.42 (s, 9H, C(CH₃)₃), 1.40 (s, 9H, C(CH₃)₃), 1.29 (s, 9H, C(CH₃)₃); MALDI-TOF: calcd for C₃₅H₆₁N₉O₂ 655.5, calcd for C₃₅H₆₁N₉O₂Na 678.5, found 656.5 [M + H]⁺, 678.5 [M + Na]⁺, 694.5 [M + K]⁺; HPLC (Water/ACN (0.1% TFA); 5% to 100% ACN in 30 min): tr = 19.29 min (Figure 16).

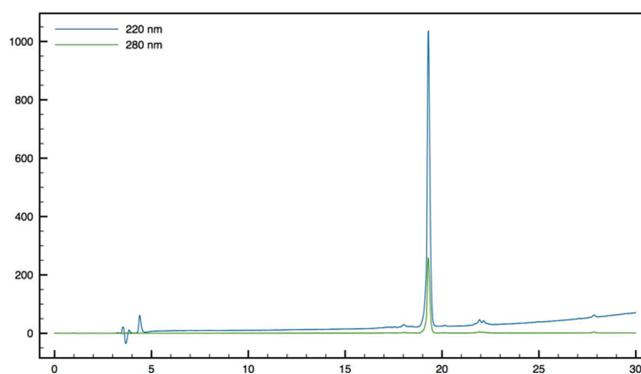


Figure 16. HPLC profile of *H*- $\beta^{3,3}$ -*h*-bis-Arg-Tbt-OMe **13**.

Gdm- $\beta^{2,2}$ -*h*-bis-Arg-Tbt-OMe **14**: HMBA-AM resin (185 mg, 0.2 mmol) was washed five times with DMF, DCM, and DMF, then allowed to swell in DMF for 30 min. Fmoc-Tbt-OH (4 eq, 0.4 mmol, 238 mg) was dissolved in dry DCM. The solution was cooled to 0 °C, and DIC (4 eq, 0.4 mmol, 60 μ L) was added. The reaction was stirred for 30 min and the solvent was then removed *in vacuo*. The resulting anhydride was dissolved in DMF and added to the resin. A solution of DMAP (0.1 eq, 0.04 mmol, 5 mg) in DMF was added and the resin was shaken for 1 h before washing with DMF, DCM, and DMF (resin loading = 0.4 mmol/g). Removal of the Fmoc protecting group was achieved by treatment

of the resin with 20% (*v:v*) piperidine in DMF 3 times for 5 min. The resin was washed five times with DMF. Fmoc- $\beta^{2,2}$ *h* bis-Orn(Boc)₂OH **2** (3 eq, 0.22 mmol, 141 mg) was dissolved in DMF (1.5 mL). HATU (1.8 eq, 0.21 mmol, 80 mg) and DIEA (4 eq, 0.88 mmol, 150 μ L) were added. The solution was added to the resin (0.07 mmol, 185 mg) and the reaction was allowed to proceed at 50 °C for 16 h. The solution was removed by filtration and the resin was washed with DMF five times. The reaction being incomplete as revealed by a Kaiser test, the same coupling procedure was repeated a second time. The resin was then treated with a 20% solution of piperidine in DMF for 5 min 3 times. Boc removal was performed by treatment with a TFA/TIS/H₂O cocktail (95:2.5:2.5) for 1 h. The free amines were then reacted with 1,3-Di-Boc-2-(trifluoromethylsulfonyl)guanidine (5 eq, 0.35 mmol, 137 mg) and NEt₃ (10 eq, 0.7 mmol, 90 μ L) in DMF overnight. The resin was filtrated and the Boc groups were removed with a TFA/TIS/H₂O cocktail (95:2.5:2.5) at rt for 3 h. After filtration, peptide **14** was cleaved from the resin using a mixture of MeOH/DMF/DIEA (5:5:1) for 16 h at 50 °C. The solution was filtrated, and solvents were evaporated. The crude product was purified by preparative RP-HPLC using a gradient of 40% to 90% MeCN in 30 min. After lyophilisation, peptide **14** was obtained as white powder with a purity of >95% (34 mg, 72% yield); ¹H NMR (300 MHz, D₂O) δ 7.36 (s, 1H, CH indole), 7.19 (s, 1H, CH indole), 4.7 (m, 1H, CH α Tbt), 3.61 (s, 3H, CO₂CH₃), 3.53 (dd, *J* = 15.3, 6.6, 1H, CH₂ β ₁ Tbt), 3.31–3.36 (m, 2H, CH₂ β ₂ Tbt and CH₂ β ϵ ₁ $\beta^{2,2}$ *h* bis-Arg), 2.88 (t, *J* = 7, 1H, CH₂ δ ₁ $\beta^{2,2}$ *h* bis-Arg), 2.85 (t, *J* = 7, 1H, CH₂ δ ₂ $\beta^{2,2}$ *h* bis-Arg), 2.83 (d, *J* = 14.5, 1H, CH₂ β ϵ ₂ $\beta^{2,2}$ *h* bis-Arg), 1.42 (s, 9H, C(CH₃)₃), 1.39 (s, 9H, C(CH₃)₃), 1.27 (s, 9H, C(CH₃)₃), 1.14–1.33 (m, 8H, CH₂ β and CH₂ γ $\beta^{2,2}$ *h* bis-Arg); MALDI-TOF: calcd for C₃₆H₆₃N₁₁O₃ 697.5, calcd for C₃₆H₆₃N₁₁O₃Na 720.5, found 698.5 [M + H]⁺, 720.4 [M + Na]⁺, 736.4 [M + K]⁺; HPLC (Water/ACN (0.1% TFA); 30% to 70% ACN in 30 min): tr = 16.5 min (Figure 17).

4.3.8. Synthesis of Fmoc-Tbt- $\beta^{2,2}$ -*h*-bis-Orn-OMe **17a** and Fmoc-Tbt- $\beta^{2,2}$ -*h*-bis-Arg-OMe **17b** (Scheme 11)

Fmoc-Tbt- $\beta^{2,2}$ -h-bis-Orn-OMe 17a: Compound **16** (42 mg, 0.042 mmol) was treated with a mixture of TFA/TIS/H₂O (95:2.5:2.5, V = 1mL) at rt for 3 h and then evaporated to dryness. The crude product was purified by preparative RP-HPLC using a gradient of 50% to 100% MeCN in 30 min. After lyophilisation compound **17a** was obtained as white powder with purity >99% (27 mg, 95% yield); ¹H NMR (300 MHz, CD₃OD) δ 7.80 (d, *J* = 7.5 Hz, 2H, CH Fmoc), 7.60 (t, *J* = 8.8 Hz, 2H, CH Fmoc), 7.37–7.42 (m, 5H, CH indole and CH Fmoc), 7.13 (d, *J* = 1.4 Hz, 1H, CH indole), 4.44 (dt, *J* = 9.8 Hz, 7.7 Hz, 1H, CH Fmoc), 4.17–4.24 (m, 3H, CH₂ Fmoc and CH α Tbt), 3.59 (d, *J* = 14.2 Hz, 1H, CH₂ β ϵ ₁ $\beta^{2,2}$ *h* bis-Arg), 3.41 (dd, *J* = 14.6 Hz, 9 Hz, 1H, CH₂ β ₁ Tbt), 3.26 (dd, *J* = 14.2 Hz, 5.8 Hz, 1H, CH₂ β ₂ Tbt), 2.88 (d, *J* = 14.2 Hz, 1H, CH₂ β ϵ ₂ $\beta^{2,2}$ *h* bis-Arg), 2.79–2.82 (m, 4H, CH₂ δ $\beta^{2,2}$ *h* bis-Arg), 1.22–1.69 (m, 35H, C(CH₃)₃, CH₂ β $\beta^{2,2}$ *h* bis-Arg and CH₂ γ $\beta^{2,2}$ *h* bis-Arg); MALDI-TOF: calcd for C₄₈H₆₇N₅O₅ 793.5, found 794.5 [M + H]⁺, 816.4 [M + Na]⁺, 832.4 [M + K]⁺; HPLC (Water/ACN (0.1% TFA); 50% to 100% ACN in 10 min: tr = 6.29 min (Figure 18).

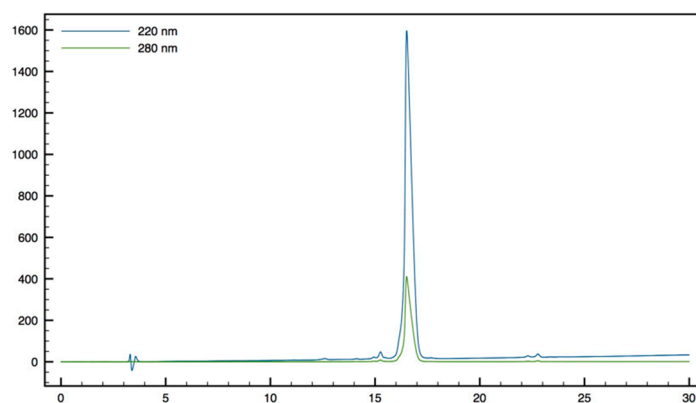
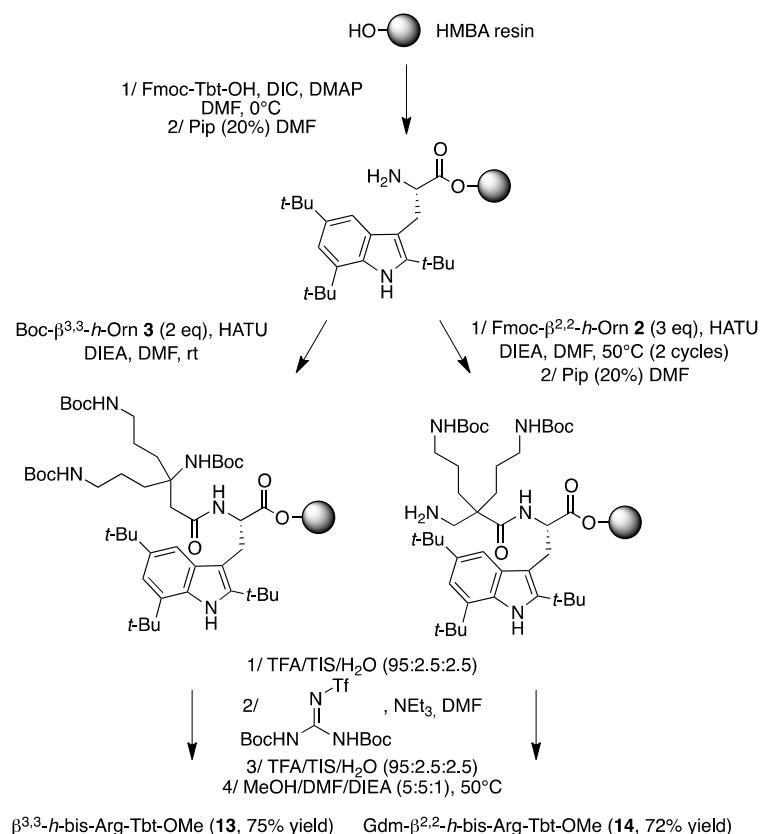
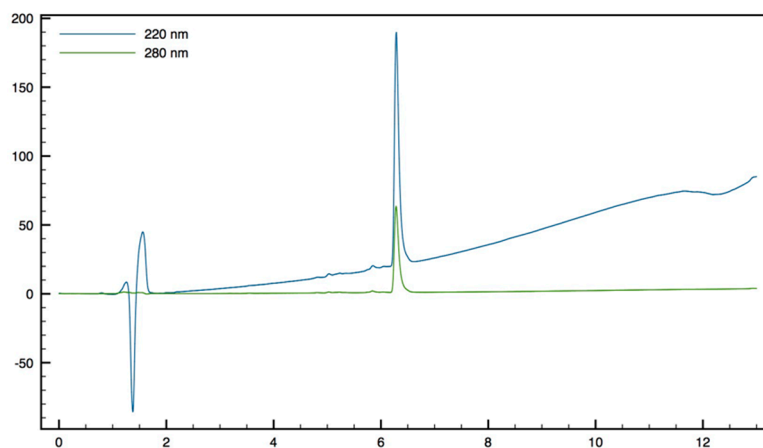


Figure 17. HPLC profile of *Gdm- $\beta^{2,2}$ -h-bis-Arg-Tbt-OMe 14*.



Scheme 10. Synthesis of peptides 13 and 14 by SPPS.

Figure 18. HPLC profile of Fmoc-Tbt-β^{2,2}-*h*-bis-Orn-OMe **17a**.

Synthesis of Fmoc-Tbt-β^{2,2}-*h*-bis-Arg-OMe **17b**

Compound **17a** (50 mg, 0.05 mmol) was dissolved in 1 mL of THF. 1,3-Di-Boc-2-(trifluoromethylsulfonyl)guanidine (51 mg, 0.13 mmol) and NEt₃ (35 μL, 0.26 mmol) were added and the reaction mixture was stirred at rt for 24 h. After evaporation of THF, a solution of TFA/TIS/H₂O (95:2.5:2.5, 2 mL) was added and the mixture was stirred at rt for 45 min. The crude product was evaporated *in vacuo* and purified by preparative RP-HPLC using a gradient of 30% to 100% MeCN in 30 min. After lyophilisation compound **17b** was obtained as white powders with purity >99% (25 mg, 57% yield); ¹H NMR (300 MHz, CD₃OD) δ 7.80 (d, *J* = 7.5 Hz, 2H, CH arom Fmoc), 7.60 (d, *J* = 7.5 Hz, 2H, CH arom Fmoc), 7.39 (t, *J* = 7.5 Hz, 2H, CH arom Fmoc), 7.33 (s, 1H, CH arom indole), 7.27 (t, *J* = 7.5 Hz, 2H, CH arom Fmoc), 7.13 (s, 1H, CH indole), 4.27–4.38 (m, 2H, CH₂ Fmoc), 4.18–4.22 (m, 2H, CH Fmoc and CH_α Tbt), 3.56 (d, *J* = 11.8 Hz, 1H, CH₂β_ε1 β^{2,2} *h* bis-Arg), 3.40 (dd, *J* = 14.6 Hz, 9.1 Hz,

1H, $CH_2\beta_1$ Tbt), 3.25 (dd, $J = 14.6$ Hz, 5.5 Hz, 1H, $CH_2\beta_2$ Tbt), 3–3.07 (m, 4H, $CH_2\delta$ $\beta^{2,2}$ *h* bis-Arg), 2.72 (d, $J = 14.3$ Hz, 2H, $CH_2\beta\epsilon_2$ $\beta^{2,2}$ *h* bis-Arg), 1.34–1.53 (m, 35H, $C(CH_3)_3$, $CH_2\beta$ $\beta^{2,2}$ *h* bis-Arg and $CH_2\gamma$ $\beta^{2,2}$ *h* bis-Arg); MALDI-TOF: calcd for $C_{50}H_{71}N_9O_5$ 877.6, found 878.4 [M + H]⁺, 916.4 [M + K]⁺; HPLC (Water/ACN (0.1% TFA); 5% to 100% ACN in 30 min: $t_r = 24.59$ min (Figure 19).

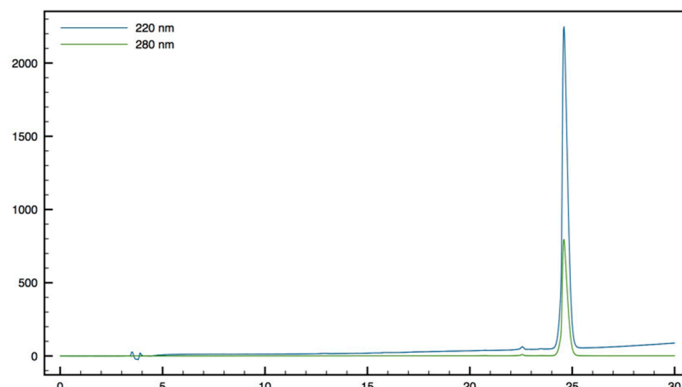
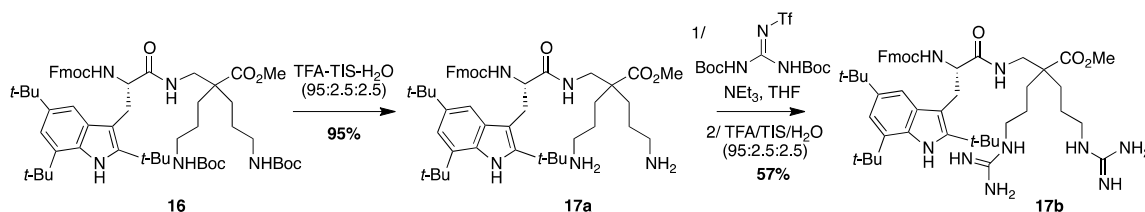


Figure 19. HPLC profile of Fmoc-Tbt- $\beta^{2,2}$ -*h*-bis-Arg-OMe 17b.



Scheme 11. Synthesis of Fmoc-Tbt- $\beta^{2,2}$ -*h*-bis-Orn-OMe 17a and Fmoc-Tbt- $\beta^{2,2}$ -*h*-bis-Arg-OMe 17b.

4.3.9. Synthesis of Fluo-Tbt- $\beta^{2,2}$ *h* bis-Orn-OMe 18 (Scheme 12)

Compound 16 (43 mg, 0.043 mmol) was dissolved in THF (1 mL) and treated with DBU (0.2 μ L, 0.0013 mmol) and octanethiol (75 μ L, 0.43 mmol) at rt for 10 min and then evaporated to dryness. The crude compound was purified by flash chromatography (DCM/MeOH/ NEt_3 , 100:0:0 to 80:20:1) affording a white powder (17 mg, 99% yield). The product was dissolved in 2 mL of THF. 2,7-di-*tert*-butylfluorene-9-carboxylic acid (17 mg, 0.05 mmol), HBTU (16 mg, 0.043 mmol), and DIEA (75 μ L, 0.43 mmol) were added and the reaction mixture was stirred at rt overnight. After evaporation of THF, a solution of TFA/TIS/ H_2O (95:2.5:2.5, 2 mL) was added and the mixture was stirred at rt for 45 min and then evaporated. The crude product was purified by preparative RP-HPLC using a gradient of 50% to 100% MeCN in 30 min. After lyophilisation compound 18 was obtained as white powder with purity >99% (24 mg, 65% yield); ¹H NMR (300 MHz, CD_3OD) δ 7.79 (s, *CH* arom fluorenyl), 7.71 (d, $J = 8$ Hz, 2H, *CH* arom fluorenyl), 7.59 (s, *CH* arom fluorenyl), 7.49 (d, $J = 8$ Hz, 2H, *CH* arom fluorenyl), 7.36 (s, 1H, *CH* indole), 7.14 (s, 1H, *CH* indole), 4.38 (dd, $J = 10$ Hz, 4 Hz, 1H, $CH\alpha$ Tbt), 3.65 (d, $J = 14$ Hz, 1H, $CH_2\beta\epsilon_1$ $\beta^{2,2}$ *h* bis-Arg), 3.56 (dd, $J = 14.8$ Hz, 10.5 Hz, 1H, $CH_2\beta_1$ Tbt), 3.39 (dd, $J = 14.8$ Hz, 4 Hz, 1H, $CH_2\beta_2$ Tbt), 2.65 (d, $J = 14.3$ Hz, 2H, $CH_2\beta\epsilon_2$ $\beta^{2,2}$ *h* bis-Arg), 2.52–2.66 (m, 2H, $CH_2\delta_1$ $\beta^{2,2}$ *h* bis-Arg), 2.38–2.45 (m, 2H, $CH_2\delta$ $\beta^{2,2}$ *h* bis-Arg), 1.30–1.53 (m, 35H, $C(CH_3)_3$, $CH_2\beta$ $\beta^{2,2}$ *h* bis-Arg and $CH_2\gamma$ $\beta^{2,2}$ *h* bis-Arg); MALDI-TOF: calcd for $C_{55}H_{81}N_5O_4$ 875.6, found 876.6 [M + H]⁺, 898.6 [M + Na]⁺, 914.6 [M + K]⁺; HPLC (Water/ACN (0.1% TFA); 45% to 100% ACN in 30 min: $t_r = 21.9$ min (Figure 20).

4.3.10. Synthesis of Np-Tbt- $\beta^{2,2}$ *h* bis-Orn-OMe 19 (Scheme 13)

Compound 16 (50 mg, 0.05 mmol) was dissolved in THF (1 mL) and treated with DBU (0.3 μ L, 0.002 mmol) and octanethiol (90 μ L, 0.5 mmol) at rt for 10 min and then evaporated to dryness. The crude compound was purified by flash chromatography (DCM/MeOH/ NEt_3 , 100:0:0 to 80:20:1)

affording a white powder (34 mg, 87% yield). This compound was dissolved in 4 mL of THF. 2-Naphtoyl chloride (9.5 mg, 0.05 mmol) and NEt_3 (14 μL , 0.1 mmol) were added and the reaction mixture was stirred at rt overnight. After evaporation of THF, a solution of TFA/TIS/ H_2O (95:2.5:2.5, 2 mL) was added and the mixture was stirred at rt for 30 min and then evaporated. The crude product was purified by preparative RP-HPLC using a gradient of 30% to 100% MeCN in 30 min. After lyophilisation compound **19** was obtained as white powder with 96% purity (22 mg, 60% yield); $^1\text{H NMR}$ (300 MHz, CD_3OD) δ 8.06 (s, 1H, CH Np), 7.91 (d, $J = 8.4$ Hz, 2H, CH Np), 7.86 (d, $J = 7.8$ Hz, 1H, CH Np), 7.75 (d, $J = 8.4$ Hz, 1H, CH Np), 7.60 (t, $J = 6.4$ Hz, 1H, CH Np), 7.56 (t, $J = 6.4$ Hz, 1H, CH Np), 7.41 (s, 1H, CH indole), 7.18 (s, 1H, CH indole), 4.57 (t, $J = 7.5$ Hz, 1H, $\text{CH}\alpha$ Tbt), 3.69 (d, $J = 14.2$, 2H, $\text{CH}_2\beta_{\epsilon_1}$ $\beta^{2,2}$ h bis-Arg), 3.63 (dd, $J = 14.7$ Hz, 8.3 Hz, 1H, $\text{CH}_2\beta_1$ Tbt), 3.48 (dd, $J = 14.7$ Hz, 6.6 Hz, 1H, $\text{CH}_2\beta_2$ Tbt), 2.99 (d, $J = 14.2$, 2H, $\text{CH}_2\beta_{\epsilon_1}$ $\beta^{2,2}$ h bis-Arg), 2.78–2.88 (m, 4H, $\text{CH}_2\delta$ $\beta^{2,2}$ h bis-Arg), 1.18–1.37 (m, 35H, $\text{C}(\text{CH}_3)_3$, $\text{CH}_2\beta$ $\beta^{2,2}$ h bis-Arg and $\text{CH}_2\gamma$ $\beta^{2,2}$ h bis-Arg); MALDI-TOF: calcd for $\text{C}_{44}\text{H}_{65}\text{N}_5\text{O}_5$ 725.5, found 726.4 $[\text{M} + \text{H}]^+$, 748.4 $[\text{M} + \text{K}]^+$, 764.4 $[\text{M} + \text{K}]^+$; HPLC (Water/ACN (0.1% TFA); 5% to 100% ACN in 30 min: $\text{tr} = 21.9$ min (Figure 21).

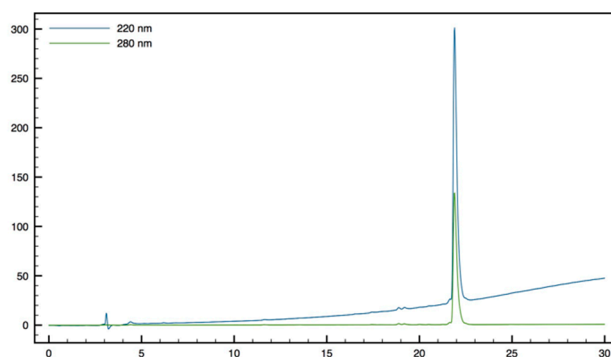
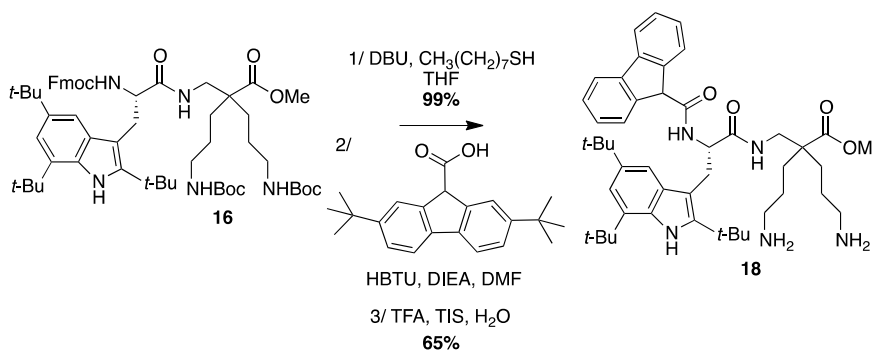


Figure 20. HPLC profile of Fluo-Tbt- $\beta^{2,2}$ h bis-Orn-OMe **18**.



Scheme 12. Synthesis of Fluo-Tbt- $\beta^{2,2}$ h bis-Orn-OMe **18**.

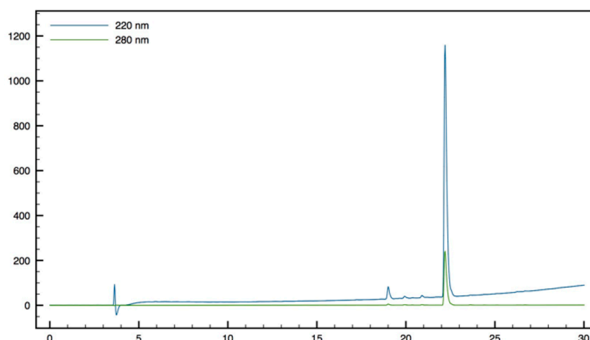
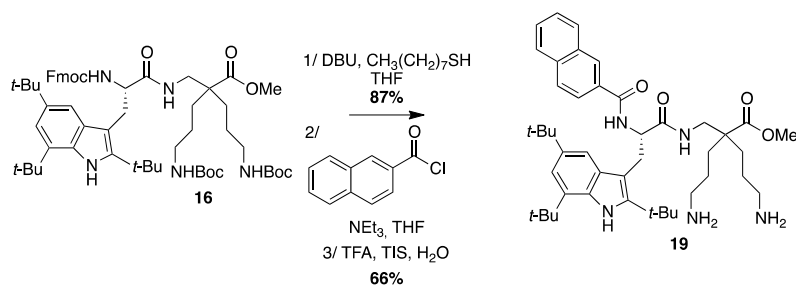


Figure 21. HPLC profile of Np-Tbt- $\beta^{2,2}$ h bis-Orn-OMe **19**.



Scheme 13. Synthesis of Np-Tbt- $\beta^{2,2}$ h bis-Orn-OMe **19**.

4.3.11. Synthesis of Tbt- $\beta^{2,2}$ h bis-Arg-OBn **20** (Scheme 14)

$\beta^{2,2}$ -*h*-bis-Orn(Boc)₂OBn **27**: Fmoc $\beta^{2,2}$ -*h*-bis-Orn(Boc)₂OH **2** (300 mg, 0.48 mmol) was dissolved in MeCN (1.7 mL). After addition of Cs₂CO₃ (188 mg, 0.58 mmol) and benzyl bromide (63 μ L, 0.53 mmol), the reaction mixture was heated at 60 °C under microwave (150W) for 10 min. The solution was filtered and evaporated to dryness. The crude compound was dissolved in AcOEt and washed with an aqueous solution of NaHCO₃ 5% followed by a solution of citric acid 5%, then dried over MgSO₄, filtered, and concentrated *in vacuo*. The crude compound was purified by flash chromatography (DCM/MeOH/NEt₃ 100:0:0.1 to 95:5:0.1) to afford a white powder (80 mg, 28% yield); ¹H NMR (300 MHz, CD₃OD) δ 7.34–7.43 (m, 5H, CH Ar), 5.17 (s, 2H, CH₂Ph), 3.01 (t, *J* = 6.8 Hz, 4H, CH₂ δ), 2.84 (s, 2H, CH₂ $\beta\epsilon$), 1.62 (dd, *J* = 9.3 Hz, 5.3 Hz, 4H, CH₂ β), 1.43 (s, 18H, C(CH₃)₃), 1.24–1.41 (m, 4H, CH₂ γ); ¹³C NMR (75 MHz, CD₃OD) δ 176.9 (C, C=O ester), 158.5 (2C, C=O carbamate), 137.5 (C, C Ar), 129.6, 129.4, 129.3 (3CH, CH Ar), 79.9 (2C, C(CH₃)₃), 67.5 (CH₂, CH₂Ph), 51.3 (CH₂, CH₂ $\beta\epsilon$), 45.5 (C, C α), 41.5 (2CH₂, CH₂ δ), 31.1 (2CH₂, CH₂ β), 28.8 (6CH₃, C(CH₃)₃), 25.3 (2CH₂, CH₂ γ); HRMS-ESI+: calcd for C₂₆H₄₃N₃O₆ 493.3152, found 494.3225 [M + H]⁺.

Fmoc-Tbt- $\beta^{2,2}$ -*h*-bis-Orn(Boc)₂OBn **28**: Fmoc-Tbt-OH (83 mg, 0.14 mmol) was dissolved in DMF (6 mL). HBTU (53 mg, 0.14 mmol) and DIEA (24 μ L, 0.14 mmol) were added and the mixture was stirred for 5 min before addition of H- $\beta^{2,2}$ -*h*-bis-Orn(Boc)₂OBn **28** (70 mg, 0.14 mmol). The reaction mixture was stirred at room temperature overnight, then diluted with Et₂O and washed with an aqueous saturated solution of NH₄Cl. The organic layer was dried over MgSO₄, filtered, and evaporated to dryness. The crude compound was purified by flash chromatography (Cy/AcOEt, 100:0 to 70:30) to afford the pure protected dipeptide as a white powder (67 mg, 45% yield). ¹H NMR (300 MHz, MeOD) δ 7.91 (s, 1H, NH indole), 7.66 (d, *J* = 7.5, 1H, CH Ar Fmoc), 7.45 (d, *J* = 7.2, 1H, CH Ar Fmoc), 7.37 (s, 1H, CH Ar indole), 7.3 (t, *J* = 7.5, 1H, CH Ar Fmoc), 7.18 (dt, *J* = 14.7 and 6.9, 1H, CH Ar Fmoc), 7.09 (s, 1H, CH indole), 5.89 (bs, 2H, NH Boc), 5.71 (bs, 1H, NH Fmoc), 4.87 (s, 2H, CH₂Ph), 4.20–4.34 (m, 3H, CH α Tbt and CH₂ Fmoc), 4.09 (t, *J* = 7.2, 1H, CH Fmoc), 3.37 (d, *J* = 14.1, 1H, CH₂ $\beta\epsilon_1$ $\beta^{2,2}$ h bis-Orn), 3.31 (d, *J* = 7.5 Hz, 2H, CH₂ β Tbt), 2.86 (m, 4H, CH₂ δ $\beta^{2,2}$ h bis-Orn), 2.55 (d, *J* = 14.1, 1H, CH₂ $\beta\epsilon_2$ $\beta^{2,2}$ h bis-Orn), 1.52 (s, 9H, C(CH₃)₃ indole), 1.47 (s, 9H, C(CH₃)₃ indole), 1.36–1.44 (m, 35H, C(CH₃)₃ indole, C(CH₃)₃ Boc, CH₂ β $\beta^{2,2}$ h bis-Orn and CH₂ γ $\beta^{2,2}$ h bis-Orn).

H-Tbt- $\beta^{2,2}$ h bis-Arg-OBn **20**: Compound **28** (68 mg, 0.064 mmol) was dissolved in DCM (~0.4 M) and an equivalent volume of TFA. The mixture was stirred at rt for 1.5 h then evaporated to dryness. The crude compound was dissolved in 4 mL of THF.

1,3-Di-Boc-2-(trifluoromethylsulfonyl)guanidine (50 mg, 0.128 mmol) and NEt₃ (500 μ L, 3.2 mmol) were added and the reaction mixture was stirred at rt for 16 h. After evaporation of THF, the crude mixture was dissolved in a 20% solution of piperidine in DCM and allowed to react for 2 h before evaporation to dryness. A solution of TFA/TIS (95:5) was added and the mixture was stirred at rt for 1.5 h. After evaporation, the crude product was purified by preparative RP-HPLC using a gradient of 20% to 90% MeCN in 30 min. After lyophilisation compound **20** was obtained as white powder with purity >99% (10 mg, 22% yield); ¹H NMR (300 MHz, CD₃OD) δ 8.36 (s, 1H, NH indole), 7.20–7.32 (m, 5H, CH Ph), 7.28 (s, 1H, CH indole), 7.15 (s, 1H, CH indole), 5.03 (d, *J* = 12 Hz, 1H, CH₂ Ph), 5.01 (d, *J* =

12 Hz, 1H, CH_2 Ph), 4.03 (t, $J = 6.1$ Hz, 1H, $CH\alpha$ Tbt), 3.60 (d, $J = 14.2$, 1H, $CH_2\beta\epsilon_1$ $\beta^{2,2}$ *h* bis-Arg), 3.42 (d, $J = 6.6$ Hz, 2H, $CH_2\beta$ Tbt), 2.97–3 (m, 4H, $CH_2\delta$ $\beta^{2,2}$ *h* bis-Arg), 2.33 (d, $J = 1.24$ Hz, 1H, $CH_2\beta\epsilon_2$ $\beta^{2,2}$ *h* bis-Arg), 1.20–1.59 (m, 35H, $C(CH_3)_3$, $CH_2\beta$ $\beta^{2,2}$ *h* bis-Arg and $CH_2\gamma$ $\beta^{2,2}$ *h* bis-Arg); MALDI-TOF: calcd for $C_{48}H_{67}N_5O_5$ 731.5, found 732.4 $[M + H]^+$, 770.3 $[M + K]^+$, 716.3 $[M + H - NH_3]^+$; HPLC (Water/ACN (0.1% TFA); 40% to 90% ACN in 10 min: $tr = 7.51$ min (Figure 22).

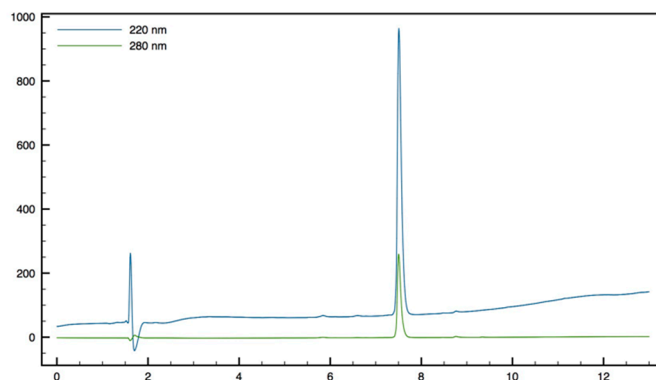
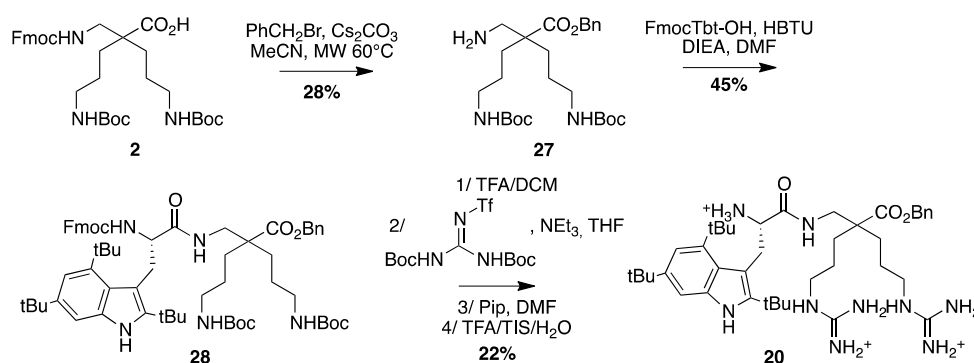


Figure 22. HPLC profile of *H*-Tbt- $\beta^{2,2}$ *h* bis-Arg-OBn 20.



Scheme 14. Synthesis of Tbt- $\beta^{2,2}$ *h* bis-Arg-OBn 20.

4.3.12. Synthesis of Tbt- $\beta^{2,2}$ *h* bis-Arg-NHBn 21 (Scheme 15)

$\beta^{2,2}$ -*h*-bis-Orn(Boc) $_2$ NHBn 29: Fmoc $\beta^{2,2}$ -*h*-bis-Orn(Boc) $_2$ OH 2 (300 mg, 0.48 mmol) was dissolved in DCM (20 mL). DCC (100 mg, 0.48 mmol), HOBT (64 mg, 0.48 mmol), DMAP (5 mg, 0.05 mmol), and benzyl amine (56 mg, 0.53 mmol) were added. The reaction mixture was stirred at rt overnight. The solution was washed with an aqueous saturated solution of NaCl, dried over $MgSO_4$, filtered, and concentrated *in vacuo*. The crude compound was purified by flash chromatography (Cy/AcOEt 100:0 to 50:50) to afford a colorless oil (251 mg, 73% yield); R_f (Cy/AcOEt, 7:3) = 0.5; 1H NMR (300 MHz, $CDCl_3$) δ 7.76 (d, $J = 7.5$ Hz, 2H, CH Ar), 7.58 (d, $J = 7.5$ Hz, 2H, CH Ar), 7.40 (t, $J = 7.5$ Hz, 2H, CH Ar), 7.25–7.33 (m, 7H, CH Ar), 6.48 (bs, 1H, NH amide), 5.47 (bs, 1H, NH Fmoc), 4.78 (bs, 2H, NH Boc), 4.36–4.42 (m, 4H, CH_2 Ph, CH_2 Fmoc), 4.15–4.20 (m, 1H, CH Fmoc), 3.36–3.38 (m, 2H, $CH_2\beta\epsilon$), 2.98–3.04 (m, 4H, $CH_2\delta$), 1.31–1.69 (m, 26H, $CH_2\beta$, $C(CH_3)_3$, $CH_2\gamma$); ^{13}C NMR (75 MHz, CD_3OD) δ 175.3 (C, C=O amide), 157.3 (C, C=O carbamate), 156.3 (C, C=O carbamate), 143.9, 141.4, 138.3 (3C, C Ar), 128.8, 127.8, 127.6, 127.1, 125.1, 120.1 (6CH, CH Ar), 79.2 (C, $C(CH_3)_3$), 66.9 (CH_2 , CH_2 Fmoc), 49.8 (C, $C\alpha$), 47.3 (CH, CH Fmoc), 44.6 (CH_2 , $CH_2\beta\epsilon$), 43.8 (CH_2 , CH_2 Ph), 40.7 (CH_2 , $CH_2\delta$), 30.8 (CH_2 , $CH_2\beta$), 29.0 (CH_3 , $C(CH_3)_3$), 24.2 (CH_2 , $CH_2\gamma$); Fmoc $\beta^{2,2}$ -*h*-bis-Orn(Boc) $_2$ NHBn (251 mg, 0.35 mmol) was dissolved in THF (6 mL). Octanethiol (600 μ L, 3.5 mmol) and DBU (1.5 μ L, 0.01 mmol) were added. The reaction mixture was stirred for 15 min then concentrated *in vacuo*. The crude compound was purified by flash chromatography (DCM/MeOH/ NEt_3 100:0:0 to 80:20:0.1) to afford 29 as a colorless oil (150 mg, 87% yield); 1H NMR (300 MHz, $CDCl_3$) δ 8.94 (bs, 2H, NH_2), 7.15–7.24 (m, 5H, CH Ar), 4.75 (bs, 2H, NH Boc), 4.33–4.35 (m, 2H, CH_2 Ph), 2.98–3.11 (m, 4H, $CH_2\delta$), 2.80 (s, 2H, $CH_2\beta\epsilon$), 1.01–1.73

(m, 26H, $CH_2\beta$, $C(CH_3)_3$, $CH_2\gamma$); ^{13}C NMR (75 MHz, CD_3OD) δ 176.3 (C, C=O amide), 156.1 (C, C=O carbamate), 139 (C, C Ar), 128.5, 127.3, 127 (3CH, CH Ar), 78.9 (C, $C(CH_3)_3$), 47.3 (C, $C\alpha$), 45.3 (CH_2 , $CH_2\beta\epsilon$), 42.9 (CH_2 , CH_2Ph), 40.8 (CH_2 , $CH_2\delta$), 31.6 (CH_2 , $CH_2\beta$), 28.4 (CH_3 , $C(CH_3)_3$), 22.4 (CH_2 , $CH_2\gamma$); HRMS-ESI+: calcd for $C_{26}H_{44}N_4O_5$ 492.3312, found 515.3199 [M + Na] $^+$.

Fmoc-Tbt- $\beta^{2,2}$ h bis-Orn(Boc) $_2$ NHBn 30: Fmoc-Tbt-OH (90 mg, 0.15 mmol) was dissolved in DMF (6 mL). HBTU (57 mg, 0.15 mmol) and DIEA (30 μ L, 0.15 mmol) were added and the mixture was stirred for 5 min before addition of H- $\beta^{2,2}$ h bis-Orn(Boc) $_2$ NHBn **29** (75 mg, 0.15 mmol). The reaction mixture was stirred at room temperature overnight, then diluted with Et_2O and washed with an aqueous saturated solution of NH_4Cl . The organic layer was dried over $MgSO_4$, filtered, and evaporated to dryness. The crude compound was purified by flash chromatography (Cy/AcOEt, 100:0 to 60:40) to afford the pure protected dipeptide **30** as a white powder (64 mg, 40% yield). 1H NMR (300 MHz, MeOD) δ 7.91 (s, 1H, NH indole), 7.65 (d, $J = 7.5$, 2H, CH Ar Fmoc), 7.40 (d, $J = 7.4$, 2H, CH Ar Fmoc), 7.35 (s, 1H, CH Ar indole), 7.28 (t, $J = 7.4$, 2H, CH Ar Fmoc), 7.03–7.20 (m, 8H, CH Ar Fmoc, CH indole, CH benzyl), 6.35 and 6.19 (2 bs, 1H, NH Amide), 5.61 (bs, 1H, NH Fmoc), 4.69 and 4.76 (2bs, 2H, NH Boc), 4.15–4.27 (m, 5H, $CH\alpha$ Tbt, CH_2 Fmoc, CH_2Ph), 4.08 (t, $J = 76.8$, 1H, CH Fmoc), 3.24–3.39 (m, 3H, $CH_2\beta_1$ Tbt, $CH_2\beta\epsilon$ $\beta^{2,2}$ h bis-Orn), 2.84–2.94 (m, 4H, $CH_2\delta$ $\beta^{2,2}$ h bis-Orn), 2.67–2.74 (m, 1H, $CH_2\beta_2$ Tbt), 1.30–1.34 (m, 53H, $C(CH_3)_3$ indole, $C(CH_3)_3$ Boc, $CH_2\beta$ $\beta^{2,2}$ h bis-Orn and $CH_2\gamma$ $\beta^{2,2}$ h bis-Orn) ^{13}C NMR (75 MHz, CD_3OD) δ 175.1 and 172.4 (C, C=O amide), 156.2 (C, C=O carbamate), 143.9, 143.6, 142.8, 142.6, 141.3, 141.2, 138.3, 132.1, 130.2, 129.8 (10C, C Ar), 128.7, 127.7, 127.4, 127.1, 125.3, 125.2, 120, 116.8, 112.1 (9CH, CH Ar), 104.5 (C, C indolyl), 79.1 (C, $C(CH_3)_3$), 67.2 (CH_2 , CH_2 Fmoc), 56.7 (CH, $CH\alpha$ Tbt), 49.2 (C, $C\alpha$ $\beta^{2,2}$ h bis-Orn), 47.1 (CH, CH Fmoc), 43.6 (CH_2 , CH_2Ph), 42.9 (CH_2 , $CH_2\beta$ Tbt), 40.7 (2 CH_2 , $CH_2\delta$ $\beta^{2,2}$ h bis-Orn), 34.9, 34.7, 33.1 (3 CH_2 , $CH_2\beta$ $\alpha\delta$ $CH_2\beta'$ $\beta^{2,2}$ h bis-Orn), 32.2, 30.9, 30.8, 30.7 (4 CH_3 , $C(CH_3)_3$), 24.2, 24.3 (2 CH_2 , $CH_2\gamma$).

H-Tbt- $\beta^{2,2}$ h bis-Arg-NHBn 21: Compound **30** (64 mg, 0.06 mmol) was dissolved in DCM (~0.4 M) and an equivalent volume of TFA containing 5% of TIS. The mixture was stirred at rt for 2 h then evaporated to dryness. The crude compound was dissolved in 4 mL of THF. 1,3-Di-Boc-2-(trifluoromethylsulfonyl)guanidine (117 mg, 0.3 mmol) and NEt_3 (80 μ L, 0.6 mmol) were added and the reaction mixture was stirred at rt for 48 h. After evaporation of THF, the crude mixture was dissolved in a 20% solution of piperidine in DCM and allowed to react for 2 h before evaporation to dryness. A solution of TFA/TIS (95:5) in DCM was added and the mixture was stirred at rt for 1.5 h. After evaporation, the crude product was purified by preparative RP-HPLC using a gradient of 40% to 100% MeCN in 30 min. After lyophilisation, compound **21** was obtained as white powder with purity >99% (20 mg, 45% yield); 1H NMR (300 MHz, CD_3OD) δ 7.32 (s, 1H, CH indole), 7.25–7.32 (m, 5H, CH arom), 7.17 (s, 1H, CH indole), 4.28 (s, 2H, CH_2Ph), 4.06 (dd, $J = 9.4$ Hz, 6.1 Hz, 1H, $CH\alpha$ Tbt), 3.44–3.56 (m, 3H, $CH_2\beta\epsilon_1$ $\beta^{2,2}$ h bis-Arg and $CH_2\beta$ Tbt), 3.11–3.17 (m, 4H, $CH_2\delta$ $\beta^{2,2}$ h bis-Arg), 2.39 (d, $J = 14$ Hz, 1H, $CH_2\beta\epsilon_2$ $\beta^{2,2}$ h bis-Arg), 1.22–1.54 (m, 35H, $C(CH_3)_3$, $CH_2\beta$ $\beta^{2,2}$ h bis-Arg and $CH_2\gamma$ $\beta^{2,2}$ h bis-Arg); MALDI-TOF: calcd for $C_{41}H_{66}N_{10}O_2$ 730.5, found 731.6 [M + H] $^+$; HPLC (Water/ACN (0.1% TFA); 40% to 100% ACN in 30 min: tr = 13.57 min (Figure 23).

4.3.13. Synthesis of Tbt- $\beta^{2,2}$ h bis-Arg-NH(CH_2) $_{13}$ CH $_3$ **22** (Scheme 16)

$\beta^{2,2}$ -h-bis-Orn(Boc) $_2$ NH(CH_2) $_{13}$ CH $_3$ 31: Fmoc $\beta^{2,2}$ h bis-Orn(Boc) $_2$ OH **2** (300 mg, 0.48 mmol) was dissolved in DCM (25 mL). DCC (109 mg, 0.53 mmol), HOBt (72 mg, 0.53 mmol), DMAP (5 mg, 0.05 mmol), and tetradecyl amine (113 mg, 0.53 mmol) were added. The reaction mixture was stirred at for 4 h. The solution was washed with brine, dried over $MgSO_4$, filtered, and concentrated *in vacuo*. The crude compound was purified by flash chromatography (Cy/AcOEt 100:0 to 50:50) to afford a colorless oil (390 mg, 99% yield); R_f (Cy/AcOEt, 1:1) = 0.76; 1H NMR (300 MHz, $CDCl_3$) δ 7.67 (d, $J = 7.3$ Hz, 2H, CH Ar), 7.51 (d, $J = 7.3$ Hz, 2H, CH Ar), 7.31 (t, $J = 7.3$ Hz, 2H, CH Ar), 7.22 (t, $J = 7.3$ Hz, 2H, CH Ar), 6.05 (bs, 1H, NH amide), 5.65 and 5.47 (2bs, 1H, NH Fmoc), 4.80 (bs, 2H, NH Boc), 4.30 (d, $J = 6.2$ Hz, 2H, CH_2 Fmoc), 4.11 (t, $J = 6.9$ Hz, 1H, CH Fmoc), 3.28 (d, $J = 6.1$ Hz,

^1H , $\text{CH}_2\beta\epsilon$ $\beta^{2,2}$ *h* bis-Orn), 3.13 (m, 2H, $\text{CH}_2\text{C}_{13}\text{H}_{27}$), 3 (m, 4H, $\text{CH}_2\delta$ $\beta^{2,2}$ *h* bis-Orn), 1.41 (m, 4H, $\text{CH}_2\gamma$ $\beta^{2,2}$ *h* bis-Orn), 1.17–1.35 (m, 46H, $\text{C}(\text{CH}_3)_3$ Boc, $(\text{CH}_2)_{12}\text{CH}_3$ and $\text{CH}_2\beta$ $\beta^{2,2}$ *h* bis-Orn), 0.8 (t, 3H, $(\text{CH}_2)_{12}\text{CH}_3$); ^{13}C NMR (75 MHz, CD_3OD) δ 175.2 (C, C=O amide), 157.3 and 156.3 (2C, C=O carbamate), 143.9 and 141.3 (C, C arom Fmoc), 127.7, 127.1, 125.1, 120 (5CH, CH arom Fmoc), 79.1 (C, $\text{C}(\text{CH}_3)_3$), 66.9 (CH_2 , CH_2 Fmoc), 49.6 (C, $\text{C}\alpha$ $\beta^{2,2}$ *h* bis-Orn), 47.2 (C, CH Fmoc), 44.6 (CH_2 , $\text{CH}_2\beta\epsilon$ $\beta^{2,2}$ *h* bis-Orn), 40.7 (CH_2 , $\text{CH}_2\text{C}_{13}\text{H}_{27}$), 39.8 (CH_2 , $\text{CH}_2\delta$ $\beta^{2,2}$ *h* bis-Orn), 33.9 (CH_2 , $\text{CH}_2\text{C}_{12}\text{H}_{25}$), 31.9 (CH_2 , $\text{CH}_2\beta$ $\beta^{2,2}$ *h* bis-Orn), 30.8 (CH_2 , $\text{CH}_2\text{C}_{11}\text{H}_{23}$), 29.72, 29.68, 29.62, 29.59, 29.39, 29.33 (CH_2 , $\text{CH}_2\text{C}_7\text{H}_{17}$), 28.4 (CH_3 , $\text{C}(\text{CH}_3)_3$), 27.1, 27.0, 24.2 (CH_2 , $(\text{CH}_2)_3\text{CH}_3$), 22.7 (CH_2 , $\text{CH}_2\gamma$ $\beta^{2,2}$ *h* bis-Orn), 14.2 (CH_3 , $(\text{CH}_2)_{13}\text{CH}_3$); HRMS-ESI+: calcd for $\text{C}_{48}\text{H}_{76}\text{N}_4\text{O}_7$ 820.5714, found 843.5606 $[\text{M} + \text{Na}]^+$. The obtained Fmoc $\beta^{2,2}$ -*h*-bis-Orn(Boc) $_{22}\text{NH}(\text{CH}_2)_{13}\text{CH}_3$ (130 mg, 0.12 mmol) was dissolved in THF (2 mL). Octanethiol (210 μL , 1.2 mmol) and DBU (0.5 μL , 0.0036 mmol) were added. The reaction mixture was stirred for 20 min then concentrated *in vacuo*. The crude compound was purified by flash chromatography (DCM/MeOH/ NEt_3 100:0:0.1 to 80:20:0.1) to afford a colorless oil (58 mg, 81% yield); ^1H NMR (300 MHz, CD_3OD) δ 3.21 (t, $J = 7.2$ Hz, 2H, $\text{CH}_2\text{C}_{12}\text{H}_{27}$), 33.04 (t, $J = 6.9$ Hz, 4H, $\text{CH}_2\delta$ $\beta^{2,2}$ *h* bis-Orn), δ 2.78 (s, 2H, $\text{CH}_2\beta'$ $\beta^{2,2}$ *h* bis-Orn), 1.32–1.58 (m, 48H, $\text{C}(\text{CH}_3)_3$ Boc, $\text{CH}_2(\text{CH}_2)_{11}\text{CH}_3$, $\text{CH}_2\beta$ $\beta^{2,2}$ *h* bis-Orn and $\text{CH}_2\gamma$ $\beta^{2,2}$ *h* bis-Orn), 0.93 (t, 3H, $J = 6.6$ Hz, $(\text{CH}_2)_{13}\text{CH}_3$); ^{13}C NMR (75 MHz, CD_3OD) δ 178.2 (C, C=O amide), 159.4 (C, C=O carbamate), 79.8 (C, $\text{C}(\text{CH}_3)_3$), 50.2 (C, $\text{C}\alpha$), 45.8 (CH_2 , $\text{CH}_2\beta'$), 41.7 (CH_2 , $\text{CH}_2\delta$), 40.4 (CH_2 , $\text{CH}_2(\text{CH}_2)_{12}\text{CH}_3$), 33.1, 31.6, 30.8, 30.5 (4 CH_2), 28.8, (6 CH_3 , $\text{C}(\text{CH}_3)_3$), 28.2, 25.3, 23.7 (CH_2), 14.5 (CH_3 , CH_2CH_3); HRMS-ESI+: calcd for $\text{C}_{33}\text{H}_{66}\text{N}_4\text{O}_5$ 598.5033, found 599.5112 $[\text{M} + \text{H}]^+$.

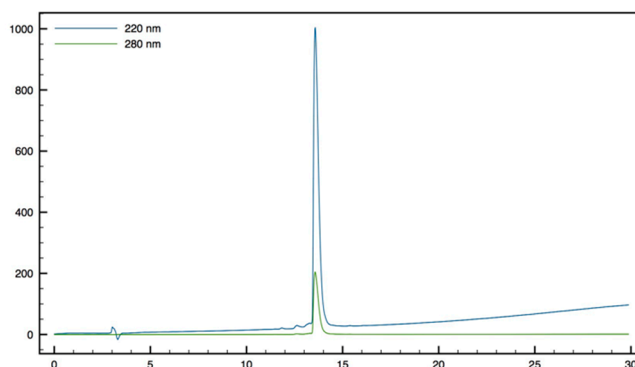
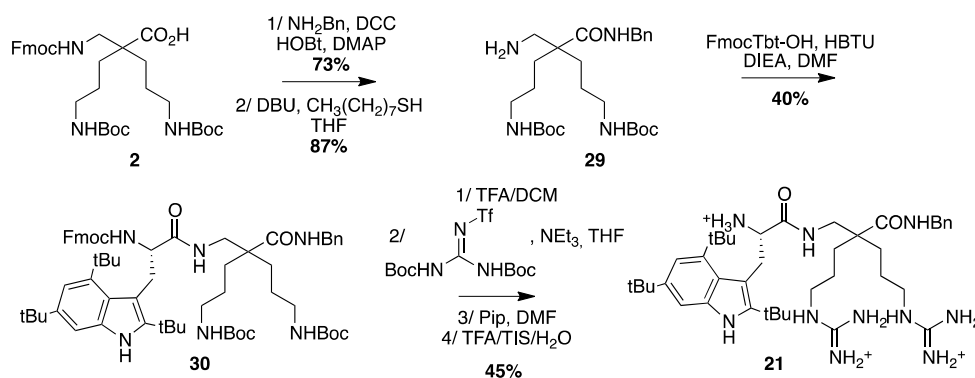


Figure 23. HPLC profile of *H*-Tbt- $\beta^{2,2}$ *h* bis-Arg-NHBn 21.



Scheme 15. Synthesis of Tbt- $\beta^{2,2}$ *h* bis-Arg-NHBn 21.

Fmoc-Tbt- $\beta^{2,2}$ -*h*-bis-Orn(Boc) $_{2}\text{NH}(\text{CH}_2)_{13}\text{CH}_3$ 32: *Fmoc*-Tbt-OH (54 mg, 0.09 mmol) was dissolved in DMF (5 mL). HBTU (34 mg, 0.09 mmol) and DIEA (20 μL , 0.09 mmol) were added and the mixture was stirred for 5 min before addition of $\beta^{2,2}$ -*h*-bis-Orn(Boc) $_{2}\text{NH}(\text{CH}_2)_{13}\text{CH}_3$ 31 (55 mg, 0.09 mmol). The reaction mixture was stirred at room temperature for 4 h, then diluted with Et_2O and washed with an aqueous saturated solution of NH_4Cl . The organic layer was dried over MgSO_4 , filtered,

and evaporated to dryness. The crude compound was purified by flash chromatography (Cy/AcOEt, 100:0 to 50:50) to afford the pure protected dipeptide as a white powder (70 mg, 66% yield). ^1H NMR (300 MHz, CDCl_3) δ 7.99 (s, 1H, NH indole), 7.23 (d, $J = 7.5$, 2H, CH Ar Fmoc), 7.50 (d, $J = 7.2$, 2H, CH Ar Fmoc), 7.43 (s, 1H, CH Ar indole), 7.38 (t, $J = 7.5$, 2H, CH Ar Fmoc), 7.24 (t, $J = 7.5$, 2H, CH Ar Fmoc), 7.17 (s, 1H, CH indole), 6.23 (bs, 1H, NH amide), 5.92 and 5.66 (2bs, 1H, NH Fmoc), 4.78 and 4.86 (2bs, 2H, NH Boc), 4.25–4.37 (m, 3H, CH_α Tbt and CH_2 Fmoc), 4.13–4.17 (m, 1H, CH Fmoc), 3.33–3.44 (m, 3H, $\text{CH}_2\beta_\epsilon$ $\beta^{2,2}$ h bis-Orn and $\text{CH}_2\beta_1$ Tbt), 3.02 (m, 6H, $\text{CH}_2\delta$ $\beta^{2,2}$ h bis-Orn and $\text{CH}_2(\text{CH}_2)_{12}\text{CH}_3$), 2.75–2.80 (m, 1H, $\text{CH}_2\beta_2$ T β \tau), 1.30–1.47 (m, 77H, 3C(CH_3) $_3$ indole, $\text{CH}_2(\text{CH}_2)_{12}\text{CH}_3$, 2C(CH_3) $_3$ Boc, 2 $\text{CH}_2\beta$ $\beta^{2,2}$ h bis-Orn and 2 $\text{CH}_2\gamma$ $\beta^{2,2}$ h bis-Orn), 0.86 (t, $J = 6.9$, 3H, (CH_2) $_{13}\text{CH}_3$) ^{13}C NMR (75 MHz, CDCl_3) δ 174.8 and 172.3 (C, C=O amide), 156.1 and 156.2 (C, C=O carbamate), 143.9, 143.6, 142.8, 142.6, 141.3, 141.2, 132.1, 130.2, 129.8 (9C, C Ar), 127.7, 127.1, 125.3, 125.2, 120, 116.8, 112.1 (7CH, CH Ar), 104.5 (C, C indolyl), 79.1 (C, C(CH_3) $_3$), 67.2 (CH_2 , CH_2 Fmoc), 56.7 (CH, CH_α T β \tau), 49.2 (C, C_α $\beta^{2,2}$ h bis-Orn), 47.1 (CH, CH F μ ox), 43 (CH_2 , $\text{CH}_2\beta$ Tbt), 40.7 (CH_2 , $\text{CH}_2\text{C}_{13}\text{H}_{29}$), 39.7 (2 CH_2 , $\text{CH}_2\delta$ $\beta^{2,2}$ h bis-Orn), 34.9 (CH_2 , $\text{CH}_2\text{C}_{12}\text{H}_{27}$), 34.8 (CH_2 , $\text{CH}_2\text{C}_{11}\text{H}_{25}$), 33.1 (CH_2 , $\text{CH}_2\text{C}_{10}\text{H}_{23}$), 32.1 (CH_3 , C(CH_3) $_3$), 32 (CH_2 , $\text{CH}_2\text{C}_9\text{H}_{21}$), 30.6 and 30.9 (2 CH_3 , C(CH_3) $_3$), 29.8, 29.7, 29.6, 29.5, 29.4, 29.3 (7 CH_2 , (CH_2) $_8\text{CH}_3$), 28.5 (2 CH_3 , C(CH_3) $_3$ Boc), 27 and 26.9 (2 CH_2 , $\text{CH}_2\beta$ $\beta^{2,2}$ h bis-Orn), 24.2 (CH_2 , $\text{CH}_2\beta_\epsilon$ $\beta^{2,2}$ h bis-Orn), 22.7 (2 CH_2 , $\text{CH}_2\gamma$), 14.2 (CH_3 , (CH_2) $_{13}\text{CH}_3$).

H-Tbt- $\beta^{2,2}$ h bis-Arg-NH(CH_2) $_{13}\text{CH}_3$ **22**: Compound **32** (52 mg, 0.045 mmol) was dissolved in DCM (3 mL) and a mixture of TFA/TIS/ H_2O (3 mL/150 μL /150 μL) as added. The solution was stirred at rt for 4 h then evaporated to dryness. The crude compound was dissolved in 4 mL of THF. 1,3-Di-Boc-2-(trifluoromethylsulfonyl)guanidine (53 mg, 0.135 mmol) and NEt_3 (40 μL , 0.27 mmol) were added and the reaction mixture was stirred at rt overnight. After evaporation of THF, the crude mixture was dissolved in a 20% solution of piperidine in DCM and allowed to react for 2 h before evaporation to dryness. A solution of TFA/TIS/ H_2O (95:2.5:2.5) in DCM was added and the mixture was stirred at rt for 3 h. After evaporation, the crude product was purified by preparative RP-HPLC using a gradient of 40% to 90% MeCN in 30 min. After lyophilisation, compound **22** was obtained as white powder with purity >99% (12 mg, 40%); ^1H NMR (300 MHz, CD_3OD) δ 8.33 (s, 1H, NH indole), 7.60 (t, $J = 5.6$ Hz, 1H, NH amide), 7.30 (d, $J = 1.5$ Hz, 1H, CH indole), 7.15 (d, $J = 1.5$ Hz, 1H, CH indole), 4.06 (dd, $J = 10.1$ Hz, 5.6 Hz, CH_α Tbt), 3.34–3.55 (m, 3H, $\text{CH}_2\beta_{\epsilon_1}$ $\beta^{2,2}$ h bis-Arg and $\text{CH}_2\beta$ Tbt), 3.11–3.17 (m, 2H, $\text{CH}_2\text{C}_{13}\text{H}_{29}$), 3.01–3.09 (m, 4H, $\text{CH}_2\delta$ $\beta^{2,2}$ h bis-Arg), 2.37 (d, $J = 14.1$ Hz, 1H, $\text{CH}_2\beta_{\epsilon_2}$ $\beta^{2,2}$ h bis-Arg), 1.68–1.84 (m, 2H, $\text{CH}_2\text{C}_{12}\text{H}_{27}$), 1.16–1.62 (m, 57H, 3C(CH_3) $_3$, (CH_2) $_{11}\text{CH}_3$, $\text{CH}_2\beta$ $\beta^{2,2}$ h bis-Arg and $\text{CH}_2\gamma$ $\beta^{2,2}$ h bis-Arg), 0.90 (t, $J = 6.7$, 3H, (CH_2) $_{13}\text{CH}_3$); MALDI-TOF: calcd for $\text{C}_{48}\text{H}_{88}\text{N}_{10}\text{O}_2$ 836.7, found 837.6 [$\text{M} + \text{H}$] $^+$, 859.6 [$\text{M} + \text{Na}$] $^+$; HPLC (Water/ACN (0.1% TFA); 50% to 100% ACN in 10 min: tr = 8.09 min (Figure 24).

4.4. Antimicrobial Assays

4.4.1. Bacterial Strains and Media

Three Gram-negative strains (*Escherichia coli* ATCC25922, *Acinetobacter baumannii* ATCC19606, and *Pseudomonas aeruginosa* ATCC29853) and three Gram-positive strains (*Staphylococcus aureus* ATCC25923, *Staphylococcus aureus* SA-1199B, and *Enterococcus faecalis* ATCC29212) were used in this study. *Staphylococcus aureus* SA-1199B is resistant to fluoroquinolones due notably to the overexpression of the membrane-associated NorA efflux pump [36].

All these strains were grown in Mueller–Hinton Broth media (MH, BioRad 69444, Mitry Mory, France) overnight at 37 °C without shaking, before being diluted in 1% Bacto Peptone water (Conda 1616.00, batch n°30927). Counting was realized on MH agar plates (MH, BioRad 64884, Mitry Mory, France). Colony forming unit (CFU) counting, used to check the bacterial density at T0 in the antibacterial activity test, was carried out by counting colonies present in 2 \times 10 μL of serial log dilutions of bacteria inoculum spotted on MH agar plates. Plates were examined for growth after one night at 37 °C.

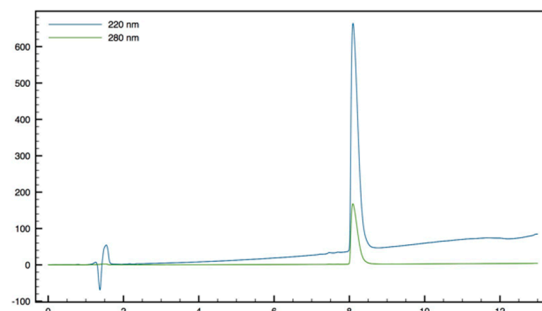
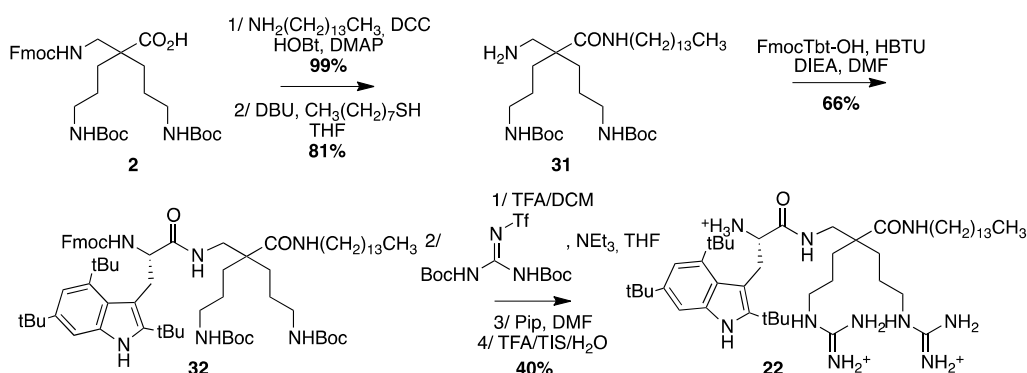


Figure 24. H-Tbt- $\beta^{2,2}$ h bis-Arg-NH(CH₂)₁₃CH₃ 22.



Scheme 16. Synthesis of Tbt- $\beta^{2,2}$ h bis-Arg-NH(CH₂)₁₃CH₃ 22.

4.4.2. Antibacterial Activity

The antibacterial activity was evaluated in 1% Bacto Peptone. First, the peptides (solubilized in H₂O or in DMSO according to their own solubility), were dispensed in a 96-wells microplate by 2-fold serial dilutions in 1% Bacto Peptone water using a handling robot (Biomek 2000, Beckman, Fullerton, CA, USA). The final volume in each well was 100 μ L. Then, 100 μ L of an overnight grown bacterial culture diluted in 1% Bacto Peptone water was added in order to reach a bacterial concentration comprised between 10⁵ and 10⁶ CFU/mL. The final range of peptide concentrations were 64, 32, 16, 8, 4, 2, 1, 0.5, 0.25, 0.125, and 0.06 μ g/mL, and the highest final concentration of DMSO or H₂O was less than 1.3% in all experiments. Growth at 37 °C without shaking was assayed using a microplate reader (DTX880, Beckman) by monitoring the absorption at 620 nm, at 0, 1, 4, 7, and 24 h. A solution of 2.6% DMSO was used as negative control, and peptide A was used as positive control. For each experiment, MICs of reference antibiotics were also measured and compared to the reported one in order to validate the assay. The minimal inhibitory concentrations (MIC) of the different peptides were defined as the lowest concentration of compound that completely inhibits cell growth during 24 h incubation. All peptides were tested at least twice in parallel.

4.5. Hemolytic Activities

Red blood cells (RBCs) were isolated from rat blood and re-suspended in PBS (4% *v/v*). RBC suspensions (100 μ L) were introduced into a 96-microwell plate and either 1 μ L (final concentration of 10 μ M) or 5 μ L (final concentration of 50 μ M)* of peptides solutions in PBS (1 mM) were added to the wells. PBS was used as negative control while a solution of 1% triton \times 100 in PBS was used as positive control. The plate was incubated for 1 h at 37 °C. After the incubation, the plate was centrifuged at 1500 rpm for 5 min. The absorbance of the supernatant 550 nm was measured and percentage of hemolysis was determined as (A – APBS)/(Atriton – A0) \times 100, where A is the absorbance of the tested well, APBS the absorbance of the negative control, and Atriton the absorbance of the positive control.

4.6. Cytotoxicity on Human SH-SYS5 Cells

The cytotoxicity of the compounds was evaluated on SH-SYS5 neuroblastoma adherent cells (Figure 7). The SH-SYS5 cells were seeded (40,000 cells per well) in 96-well microplates the day before, then incubated at 37 °C, with 0, 1, 10, 50, or 100 µM compounds in RPMI for 2 h. The cell-counting kit solution was used as indicated by the supplier (Dojindo Laboratories). Absorbance at 450 nm (and reference at 620 nm) is directly related to the number of living cells. Experiments were done in triplicates and repeated two-times independently. Results are normalized to the control cells, in the absence of any compound.

4.7. In Vivo Experiments

Mice were bred and maintained at the mouse facilities of the Bichat Medical School campus. All experiments were performed in accordance with the French Council of Animal Care guidelines and national ethical guidelines of INSERM Animal Care Committee (Animal Use Protocol number 75-1596).

4.8. Cecal Ligation and Puncture (CLP)

Bl6 mice (only male 12 weeks old) were anesthetized and the cecum exposed by a 1 cm midline incision on the abdomen. The distal half of the cecum was ligated with a 5-0 silk suture and punctured with a 21-gauge needle. The cecum was replaced, and 1 ml of sterile saline injected into the peritoneal cavity. The incision was closed using surgical sutures. Mice were monitored every 8 h for the first 3 days and then every 12 h until death or day 7, when they were euthanized. For the peptide **11** treatment, 1 µg/g of mice (on average 20 g) was injected (intraperitoneal injection) during the surgical suture at the end of the CLP procedure.

4.9. Peptide Hydrophobicity

Analytical HPLC on C18 column (Higgins RS 1046 D183, 100*4.6 mm) using as eluent a 5% to 100% gradient of MeCN containing 0.1% TFA in water containing 0.1% TFA, in 30 min, and UV detection was done at 220 and 280 nm.

4.10. Stability of Peptide in Human Serum

To a mixture of 250 µL of human serum and 750 µL of RPMI 1640 were added 20 µL of the peptide solution at 10 mg/mL. The mixture was incubated at 37 °C. Aliquots of 100 µL were removed from the medium at different time, mixed with 100 µL of ethanol and 5 µL of 1M NaOH, and incubated at 4 °C for at least 15 min to precipitate all the serum proteins. After centrifugation at 12,000 rpm for 2 min, 50 µL of the supernatant were injected in HPLC with a linear gradient from 5% to 50% ACN [0.1% (v/v) TFA in acetonitrile] in aqueous 0.1% (v/v) TFA. The relative concentrations of the remaining soluble peptides were analyzed by the integration of the absorbance at 220 nm as a function of retention time.

To ensure the serum activity, the peptide 4NGG [37] is used as positive control (Figure 25):

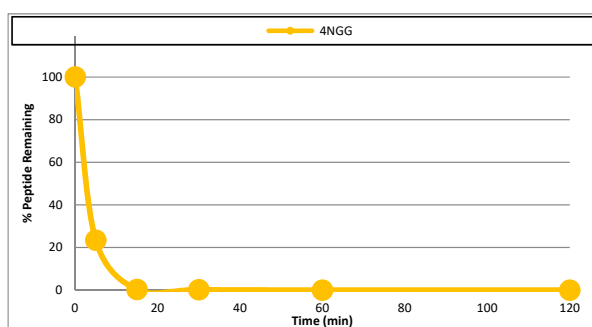


Figure 25. Serum activity evaluated with the 4NGG peptide degraded in 15 min.

5. Patents

The patent application WO2014191392 A1 (PCT/EP2014/060917) included results from this paper. The authors declare that no other competing interest exist.

Supplementary Materials: The following are available online. ¹H and ¹³C NMR Spectra of all compounds.

Author Contributions: H.B. performed amino acids, peptides syntheses and metabolic stability assay under the supervision of R.M. and P.K. A.H., C.G.-E. performed the antimicrobial assays under the supervision of C.J. C.B. and H.B. performed the cytotoxicity assays under the supervision of S.S. E.P. performed the in vivo assays under the supervision of P.L. F.B. and C.L. performed the study of Interaction with membrane model. P.K. and R.M. wrote the manuscript with the assistance of the others authors. P.K. designed the AMPs and led the project. All authors have given approval to the final version of the manuscript.

Funding: H.B. was recipient of a MERS fellowship from the french Ministère de l'Enseignement Supérieure et de la Recherche. P.K. is grateful to SATT-Lutech and DGRIT (Sorbonne-Université) for financial and logistic supports in patent filing.

Conflicts of Interest: The authors declare no conflict of interest.

References

1. Jones, D. The antibacterial lead discovery challenge. *Nat. Rev. Drug Discov.* **2010**, *9*, 751–752.
2. Bax, B.D.; Chan, P.F.; Eggleston, D.S.; Fosberry, A.; Gentry, D.R.; Gorrec, F.; Giordano, I.; Hann, M.M.; Hennessy, A.; Hibbs, M.; et al. Type IIA topoisomerase inhibition by a new class of antibacterial agents. *Nature* **2010**, *466*, 935–940. [[CrossRef](#)] [[PubMed](#)]
3. Fjell, C.D.; Hiss, J.A.; Hancock, R.E.W.; Schneider, G. Designing antimicrobial peptides: Form follows function. *Nat. Rev. Drug Discov.* **2011**, *1*, 37–51.
4. Uggerhøj, L.E.; Poulsen, T.J.; Munk, J.K.; Fredborg, M.; Sondergaard, T.E.; Frimodt-Møller, N.; Hansen, P.R.; Wimmer, R. Rational design of alpha-helical antimicrobial peptides: Do's and don'ts. *ChemBioChem* **2015**, *16*, 242–253. [[CrossRef](#)] [[PubMed](#)]
5. Shai, Y. Mode of action of membrane active antimicrobial peptides. *Biopolymers* **2002**, *66*, 236–248. [[CrossRef](#)] [[PubMed](#)]
6. Tew, G.N.; Scott, R.W.; Klein, M.L.; DeGrado, W.F. De Novo Design of Antimicrobial Polymers, Foldamers, and Small Molecules: From Discovery to Practical Applications. *Acc. Chem. Res.* **2010**, *43*, 30–39. [[CrossRef](#)]
7. Ramesh, S.; Govender, T.; Kruger, H.G.; de la Torre, B.G.; Albericio, F. Short AntiMicrobial Peptides (SAMPs) as a class of extraordinary promising therapeutic agents. *J. Pept. Sci.* **2016**, *22*, 438–451. [[CrossRef](#)]
8. Teng, P.; Nimmagadda, A.; Su, M.; Hong, Y.; Shen, N.; Li, C.; Tsai, L.-Y.; Cao, J.; Li, Q.; Cai, J. Novel bis-cyclic guanidines as potent membrane-active antibacterial agents with therapeutic potential. *Chem Commun.* **2017**, *53*, 11948–11951. [[CrossRef](#)]
9. Niu, Y.; Wang, M.; Yafei Cao, Y.; Nimmagadda, A.; Hu, J.; Wu, Y.; Cai, J.; Ye, X.-S. Rational Design of Dimeric Lysine N-Alkylamide as Potent and Broad Spectrum Antibacterial Agents. *J. Med. Chem.* **2018**, *61*, 2865–2874. [[CrossRef](#)]
10. Aussedat, B.; Dupont, E.; Sagan, S.; Joliot, A.; Lavielle, S.; Chassaing, G.; Burlina, F. Modifications in the chemical structure of Trojan carriers: Impact on cargo delivery. *Chem. Commun.* **2008**, 1398–1400. [[CrossRef](#)]
11. Seebach, D.; Abele, S.; Sifferlen, T.; Hänggi, M.; Gruner, S.; Seiler, P. Disubstituted $\beta^{2,2}$ and $\beta^{3,3}$ amino Acids. A Turn Motif for β -peptides. *Helv. Chim. Acta* **1998**, *81*, 2218–2243. [[CrossRef](#)]
12. Yu, J.-S.; Noda, H.; Shibasaki, M. Quaternary $\beta^{2,2}$ -Amino Acids: Catalytic Asymmetric Synthesis and Incorporation into Peptides by Fmoc-Based Solid-Phase Peptide Synthesis. *Angew. Chem. Int. Ed.* **2018**, *57*, 818–822. [[CrossRef](#)] [[PubMed](#)]
13. Basuroy, K.; Rajagopal, A.; Raghothama, S.; Shamala, N.; Balaram, P. β -Turn analogues in model $\alpha\beta$ -hybrid peptides: Structural characterization of peptides containing $\beta(2,2)$ Ac6c and $\beta(3,3)$ Ac6c residues. *Chem. Asian J.* **2012**, *7*, 1671–1678. [[CrossRef](#)] [[PubMed](#)]
14. García-González, I.; Mata, L.; Corzana, F.; Jiménez-Osés, G.; Avenoza, A.; Busto, J.H.; Peregrina, J.M. Synthesis and conformational analysis of hybrid α/β -dipeptides incorporating S-glycosyl- $\beta(2,2)$ -amino acids. *Chemistry* **2015**, *21*, 1156–1168. [[CrossRef](#)]

15. Hansen, T.; Ausbacher, D.; Flaten, G.E.; Havelkova, M.; Strøm, M.B. Synthesis of cationic antimicrobial $\beta(2,2)$ -amino acid derivatives with potential for oral administration. *J. Med. Chem.* **2012**, *54*, 858–868. [[CrossRef](#)]
16. Tørfoss, V.; Ausbacher, D.; de A. Cavalcanti-Jacobsen, C.; Hansen, T.; Brandsdal, B.-O.; Havelkova, M.; Strøm, M.B. Synthesis of anticancer heptapeptides containing a unique lipophilic $\beta(2,2)$ -amino acid building block. *J. Pept. Sci.* **2012**, *18*, 170–176. [[CrossRef](#)]
17. Hansen, T.; Ausbacher, D.; Zachariassen, Z.G.; Anderssen, T.; Havelkova, M.; Strøm, M.B. Anticancer activity of small amphipathic $\beta^2,^2$ -amino acid derivatives. *Eur. J. Med. Chem.* **2012**, *58*, 22–29. [[CrossRef](#)] [[PubMed](#)]
18. Saidi, M.R.; Azizi, N.; Akbari, E.; Ebrahimi, F. LiCO₄/Et₃N: Highly efficient and active catalyst for selective Michael addition of active methylene compounds under solvent-free condition. *J. Mol. Catal. A Chem.* **2008**, *292*, 44–48. [[CrossRef](#)]
19. Strøm, M.B.; Rekdal, Ø.; Svendsen, J.S. Antimicrobial activity of short arginine- and tryptophan-rich peptides. *J. Pept. Sci.* **2002**, *8*, 431–437. [[CrossRef](#)] [[PubMed](#)]
20. Strøm, M.B.; Haug, B.E.; Skar, M.L.; Stensen, W.; Stiberg, T.; Svendsen, J.S. The pharmacophore of short cationic antibacterial peptides. *J. Med. Chem.* **2003**, *46*, 1567–1570. [[CrossRef](#)] [[PubMed](#)]
21. Haug, B.E.; Stensen, W.; Stiberg, T.; Svendsen, J.S. Bulky nonproteinogenic amino acids permit the design of very small and effective cationic antibacterial peptides. *J. Med. Chem.* **2004**, *47*, 4159–4162. [[CrossRef](#)] [[PubMed](#)]
22. Haug, B.E.; Stensen, W.; Kalaaji, M.; Rekdal, Ø.; Svendsen, J.S. Synthetic antimicrobial peptidomimetics with therapeutic potential. *J. Med. Chem.* **2008**, *51*, 4306–4314. [[CrossRef](#)] [[PubMed](#)]
23. Isaksson, J.; Brandsdal, B.O.; Engqvist, M.; Flaten, G.E.; Svendsen, J.S.M.; Stensen, W. A synthetic antimicrobial peptidomimetic (LTX 109): Stereochemical impact on membrane disruption. *J. Med. Chem.* **2011**, *54*, 5786–5795. [[CrossRef](#)] [[PubMed](#)]
24. Sharma, R.K.; Reddy, R.P.; Tegge, W.; Jain, R. Discovery of Trp-His and His-Arg analogues as new structural classes of short antimicrobial peptides. *J. Med. Chem.* **2009**, *52*, 7421–7431. [[CrossRef](#)] [[PubMed](#)]
25. Hansen, T.; Alst, T.; Havelkova, M.; Strøm, M.B. Antimicrobial activity of small beta-peptidomimetics based on the pharmacophore model of short cationic antimicrobial peptides. *J. Med. Chem.* **2010**, *53*, 595–606. [[CrossRef](#)] [[PubMed](#)]
26. Bremner, J.B.; Keller, P.A.; Pyne, S.G.; Boyle, T.P.; Brkic, Z.; David, D.M.; Garas, A.; Morgan, J.; Robertson, M.; Somphol, K.; et al. Binaphthyl-based dicationic peptoids with therapeutic potential. *Angew. Chem. Int. Ed.* **2010**, *49*, 537–540. [[CrossRef](#)] [[PubMed](#)]
27. Rekdal, Ø.; Haug, B.E.; Kalaaji, M.; Hunter, H.N.; Lindin, I.; Israelsson, I.; Solstad, T.; Yang, N.; Brandl, M.; Mantzilas, D.; Vogel, H.J. Relative spatial positions of tryptophan and cationic residues in helical membrane-active peptides determine their cytotoxicity. *J. Biol. Chem.* **2012**, *287*, 233–244. [[CrossRef](#)] [[PubMed](#)]
28. Thennarasu, S.; Lee, D.-K.; Tan, A.; Prasad Kari, U.; Ramamoorthy, A. Antimicrobial activity and membrane selective interactions of a synthetic lipopeptide MSI-843. *Biochim. Biophys. Acta* **2005**, *1711*, 49–58. [[CrossRef](#)] [[PubMed](#)]
29. Das, S.; Ben Haj Salah, K.; Wenger, E.; Martinez, J.; Kotarba, J.; Andreu, V.; Ruiz, N.; Savini, F.; Stella, L.; Didierjean, C.; et al. Enhancing the Antimicrobial Activity of Alamethicin F50/5 by Incorporating N-terminal Hydrophobic Triazole Substituents. *Chemistry* **2017**, *23*, 17964–17972. [[CrossRef](#)] [[PubMed](#)]
30. Ladokhin, A.S.; Jayasinghe, S.; White, S.H. How to measure and analyze tryptophan fluorescence in membranes properly, and why bother? *Anal. Biochem.* **2000**, *285*, 235–245. [[CrossRef](#)] [[PubMed](#)]
31. Killian, J.A.; Keller, R.C.A.; Struyve, M.; De Kroon, A.; Tommassen, J.; De Kruijff, B. Tryptophan fluorescence study on the interaction of the signal peptide of the Escherichia coli outer membrane protein PhoE with model membranes. *Biochemistry* **1990**, *29*, 8131–8137. [[CrossRef](#)] [[PubMed](#)]
32. Pinheiro da Silva, F.; Aloulou, M.; Skurnik, D.; Benhamou, M.; Andremont, A.; Velasco, I.T.; Chiamolera, M.; Verbeek, J.S.; Launay, P.; Monteiro, R.C. CD16 promotes Escherichia coli sepsis through an FcR gamma inhibitory pathway that prevents phagocytosis and facilitates inflammation. *Nat. Med.* **2007**, *13*, 1368–1374. [[CrossRef](#)] [[PubMed](#)]
33. Svenson, J.; Karstad, R.; Flaten, G.E.; Brandsdal, B.-O.; Brandl, M.; Svendsen, J.S. Altered activity and physicochemical properties of short cationic antimicrobial peptides by incorporation of arginine analogues. *Mol. Pharm.* **2009**, *6*, 996–1005. [[CrossRef](#)] [[PubMed](#)]

34. Bisello, A.; Sala, S.; Tonello, A.; Signor, G.; Melotto, E.; Mammi, S.; Peggion, E. Conformation and interactions of all-D-, retro-all-D- and retro-bombolitin III analogues in aqueous solution and in the presence of detergent micelles. *Int. J. Biol. Macromol.* **1995**, *17*, 273–282. [[CrossRef](#)]
35. Basuroy, K.; Karuppiyah, V.; Shamala, N.; Balaram, P. The Structural Characterization of Folded Peptides Containing the Conformationally Constrained β^2 -Amino Acid Residue $\beta^{2,2}$ Ac₆c. *Helv. Chim.* **2012**, *95*, 2589–2603. [[CrossRef](#)]
36. Sabatini, S.; Gosetto, F.; Manfroni, G.; Tabarrini, O.; Kaatz, G.W.; Patel, D.; Cecchetti, V. Evolution from a natural flavones nucleus to obtain 2-(4-Propoxyphenyl)quinoline derivatives as potent inhibitors of the *S. aureus* NorA efflux pump. *J. Med. Chem.* **2011**, *54*, 5722–5736. [[CrossRef](#)] [[PubMed](#)]
37. Denèfle, T.; Boulet, H.; Herbi, L.; Newton, C.; Martinez-Torres, A.C.; Guez, A.; Pramil, E.; Quiney, C.; Pourcelot, M.; Levasseur, M.D.; et al. Thrombospondin-1 Mimetic Agonist Peptides Induce Selective Death in Tumor Cells: Design, Synthesis, and Structure-Activity Relationship Studies. *J. Med. Chem.* **2016**, *59*, 8412–8421. [[CrossRef](#)] [[PubMed](#)]

Sample Availability: Sample of the compound **11** is available from the authors.



© 2019 by the authors. Licensee MDPI, Basel, Switzerland. This article is an open access article distributed under the terms and conditions of the Creative Commons Attribution (CC BY) license (<http://creativecommons.org/licenses/by/4.0/>).